

## Accepted Manuscript

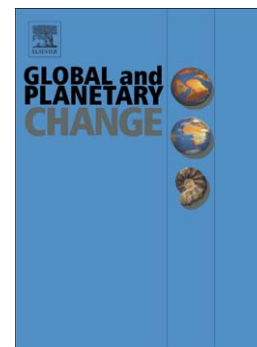
New constraints on the timing of West Antarctic Ice Sheet retreat in the eastern Amundsen Sea since the Last Glacial Maximum

James A. Smith, Claus-Dieter Hillenbrand, Gerhard Kuhn, Johann Phillip Klages, Alastair G.C. Graham, Robert D. Larter, Werner Ehrmann, Steven G. Moreton, Steffen Wiers, Thomas Frederichs

PII: S0921-8181(14)00148-9  
DOI: doi: [10.1016/j.gloplacha.2014.07.015](https://doi.org/10.1016/j.gloplacha.2014.07.015)  
Reference: GLOBAL 2155

To appear in: *Global and Planetary Change*

Received date: 3 March 2014  
Revised date: 29 July 2014  
Accepted date: 30 July 2014



Please cite this article as: Smith, James A., Hillenbrand, Claus-Dieter, Kuhn, Gerhard, Klages, Johann Phillip, Graham, Alastair G.C., Larter, Robert D., Ehrmann, Werner, Moreton, Steven G., Wiers, Steffen, Frederichs, Thomas, New constraints on the timing of West Antarctic Ice Sheet retreat in the eastern Amundsen Sea since the Last Glacial Maximum, *Global and Planetary Change* (2014), doi: [10.1016/j.gloplacha.2014.07.015](https://doi.org/10.1016/j.gloplacha.2014.07.015)

This is a PDF file of an unedited manuscript that has been accepted for publication. As a service to our customers we are providing this early version of the manuscript. The manuscript will undergo copyediting, typesetting, and review of the resulting proof before it is published in its final form. Please note that during the production process errors may be discovered which could affect the content, and all legal disclaimers that apply to the journal pertain.

# NEW CONSTRAINTS ON THE TIMING OF WEST ANTARCTIC ICE SHEET RETREAT IN THE EASTERN AMUNDSEN SEA SINCE THE LAST GLACIAL MAXIMUM

James A. Smith<sup>1\*</sup>, Claus-Dieter Hillenbrand<sup>1</sup>, Gerhard Kuhn<sup>2</sup>, Johann Phillip Klages<sup>2</sup>, Alastair G.C. Graham<sup>1,3</sup>, Robert D. Larter<sup>1</sup>, Werner Ehrmann<sup>4</sup>, Steven G. Moreton<sup>5</sup>, Steffen Wiers, Thomas Frederichs<sup>6</sup>

<sup>1</sup>*British Antarctic Survey, High Cross, Madingley Road, Cambridge, CB3 0ET, UK.*

<sup>2</sup>*Alfred-Wegener-Institut Helmholtz-Zentrum für Polar- und Meeresforschung, P.O. Box 120161, D-27515 Bremerhaven, Germany*

<sup>3</sup>*College of Life and Environmental Sciences, University of Exeter, Exeter EX4 4RJ, UK*

<sup>4</sup>*Institute for Geophysics and Geology, University of Leipzig, Talstrasse 35, D-04103 Leipzig, Germany.*

<sup>5</sup>*NERC Radiocarbon Facility (Environment), East Kilbride, UK*

<sup>6</sup>*Department of Geosciences, University of Bremen, P.O. Box 330440, D-28334 Bremen, Germany*

Corresponding author:

Dr. James Smith

phone: +44 (0)1223 2212229

fax: +44 (0)1223 221646

email: jaas@bas.ac.uk

**Abstract**

Glaciers flowing into the Amundsen Sea Embayment (ASE) account for >35% of the total discharge of the West Antarctic Ice Sheet (WAIS) and have thinned and retreated dramatically over the past two decades. Here we present detailed marine geological data and an extensive new radiocarbon dataset from the eastern ASE in order to constrain the retreat of the WAIS since the Last Glacial Maximum (LGM) and assess the significance of these recent changes. Our dating approach, relying mainly on the acid insoluble organic (AIO) fraction, utilises multi-proxy analyses of the sediments to characterise their lithofacies and determine the horizon in each core that would yield the most reliable age for deglaciation. In total, we dated 69 samples and show that deglaciation of the outer shelf was underway before 20,600 calibrated years before present (cal. yr BP), reaching the mid-shelf by 13,575 cal. yr BP and the inner shelf to within c.150 km of the present grounding line by 10,615 cal. yr BP. The timing of retreat is broadly consistent with previously published radiocarbon dates on biogenic carbonate from the eastern ASE as well as AIO  $^{14}\text{C}$  ages from the western ASE and provides new constraints for ice sheet models. The overall retreat trajectory – slow on the outer shelf, more rapid from the middle to inner shelf – clearly highlights the importance of reverse bedslopes in controlling phases of accelerated grounding line retreat. Despite revealing these broad scale trends, the current dataset does not capture detailed changes in ice flow, such as stillstands during grounding line retreat (i.e., deposition of grounding zone wedges) and possible readvances as depicted in the geomorphological record.

*Keywords:*  $^{14}\text{C}$  dating, Pine Island Glacier, grounding zone wedge, ice shelf, ice sheet modelling

## 1. Introduction

Assessing the duration, timing and forcing of past ice sheet retreat is essential if we are to fully understand the controls on recent ice sheet changes and predict its future behaviour (Bentley *et al.* in press). Accurately dated 'retreat trajectories' are particularly needed for the Amundsen Sea sector of the West Antarctic Ice Sheet (WAIS), where glaciers have accelerated and thinned dramatically and now account for >35% of its total discharge (Rignot, 2008; Rignot *et al.*, 2008; Shepherd *et al.*, 2012). These changes have been accompanied by rapid inland retreat of the grounding line (GL) of Pine Island Glacier (PIG) (Joughin *et al.*, 2010) and Thwaites Glacier (Tinto and Bell, 2011) raising concern that large-scale collapse is possible on human timescales (Katz and Worster, 2010; Gladstone *et al.*, 2012; Favier *et al.* 2014; Joughin *et al.* 2014). Complete collapse of the glaciers in this region would raise global sea level by ~1.5 m and although this remains a possibility, recent estimates suggest that melting of PIG alone will contribute 3.5-10 mm over the next 20 years (Favier *et al.*, 2014) The coherent thinning of glaciers across the Amundsen Sea Embayment (ASE) has been attributed to melting of the floating ice shelves by warm Circumpolar Deep Water (CDW) upwelling onto the continental shelf (Jacobs *et al.*, 1996; 2011; Shepherd *et al.*, 2004; Walker *et al.*, 2008; Jacobs *et al.*, 2011), with modelling studies showing that this imbalance is propagated upstream thus affecting the whole ice stream system (Payne *et al.*, 2004).

This work has focussed attention on when the imbalance was initiated, and whether it represents a recent change related to variations in the delivery of CDW onto the shelf (Thoma *et al.*, 2008; Steig *et al.*, 2012) or some other internal or external trigger (i.e., topography, ice dynamics) that occurred sometime in the recent geological past, e.g. following deglaciation from the LGM (19-23 kyr). According to Larter *et al.* (in press) the rates of change currently observed in the ASE are too high to be a simple continuation of deglaciation from the LGM as such high modern retreat rates (i.e.,  $0.95 \pm 0.09$  km yr<sup>-1</sup> between 1992-2011; Park *et al.* 2013) would have resulted in deglaciation of the entire continental shelf within 500 years, which is in conflict with recent marine geological data (e.g., Smith *et al.*, 2011). There is also a growing body of geomorphological evidence that ice sheet retreat following the LGM was oscillatory with periods of rapid change punctuated by periods of relative stability (Graham *et al.*, 2010; Jakobsson *et al.* 2011).

However, despite recent progress in dating the timing of ice sheet retreat in the ASE (see recent review by Larter *et al.*, in press) much of the detail, including oscillations in GL positions and the duration of still-stands, is yet to be fully resolved. This reflects two

fundamental, but persistent problems: (1) lack of data from key areas of the shelf owing to the logistical challenges of working in the ASE, both in terms of distance from Antarctic research stations and persistent sea ice coverage; and (2) significant challenges associated with dating marine sediments on the Antarctic continental shelf. In this context, the scarcity of calcareous (micro-)fossils in combination with the large and variable input of reworked fossil organic carbon from the hinterland has hampered efforts to establish a detailed retreat histories, especially when attempting to constrain the subglacial to glacier-proximal transition. Notwithstanding these problems, recent studies from the Bellingshausen Sea and western ASE shelf have demonstrated that with a careful sampling strategy guided by detailed sedimentological information, reliable deglacial chronologies can be produced using the acid insoluble organic (AIO) fraction (Hillenbrand *et al.* 2010a; Smith *et al.*, 2011). This approach requires a local reservoir correction, achieved by dating the surface sediments (usually obtained from box cores) and subtracting this age from down-core ages (cf. Andrews *et al.*, 1999), alongside sufficient down-core dates to identify major steps in  $^{14}\text{C}$  age progression (so-called  $^{14}\text{C}$  dog-legs). In the western ASE the validity of this approach has been verified by other independent dating methods (relative palaeomagnetic intensity (RPI) and paired carbonate-AIO dating (e.g., Hillenbrand *et al.*, 2010b; Smith *et al.*, 2011) illustrating that with careful sample selection, reliable deglacial chronologies can be obtained even when biogenic carbonate is sparse.

The current paper presents a new AIO-based deglacial chronology for the eastern ASE, which complements and significantly expands upon the largely carbonate-based deglacial ages recently published by Kirshner *et al.* (2012) and Hillenbrand *et al.* (2013) and provides a key dataset for the ice sheet modelling community. Whilst our new deglacial framework further demonstrates the utility of a careful AIO-based dating strategy, the lack of core material from key areas as well as a highly variable input of reworked fossil organic carbon, particularly in the central trough continues to represent challenges. We discuss these limitations in the context of geomorphological data which shows a stepped retreat across the outer to mid-shelf and summarize what we can (and cannot) say about the trajectory of ice sheet retreat in the eastern ASE.

### 1.1. Study area and previous work

The glacial history of the ASE has recently been reviewed by Larter *et al.* (in press) so is only briefly described here. The gross bathymetry of the ASE is characterised by cross-shelf bathymetric troughs which mark the former pathways of ice streams that advanced to, or close to, the continental shelf edge during the LGM (Fig. 1) (Evans *et al.*, 2006; Larter *et al.*,

2009; Nitsche *et al.*, 2007; Graham *et al.*, 2009; 2010; Kirshner *et al.*, 2012). Geomorphological mapping of the inner-mid shelf showed that the Pine Island and Thwaites glaciers converged to a single palaeo ice stream (PITPIS) as the WAIS advanced across the shelf (Fig. 1). PITPIS was topographically constrained on the inner to mid-shelf by the main Pine Island Trough (PIT). The main trough then bifurcates on the outer shelf into western and eastern branches referred to as Pine Island Trough West (PITW) and East (PITE) (Evans *et al.*, 2006; Graham *et al.*, 2010; Jakobsson *et al.*, 2012). Streaming ice was also concentrated along the eastern coastline (Cosgrove-Abbot Trough) (Fig. 1) with a connection to ice flowing out of Ferrero Bay in the south (Fig.1) but separated from PITPIS by an area of slower moving ice around Burke Island (Klages *et al.*, 2013; Klages, 2014). Well-developed GZWs occur along the PITE and main trough axis (GZW1-5; Graham *et al.*, 2010) with extensions in the Abbott-Cosgrove troughs (GZWa,b; Klages, 2014; Kellogg & Kellogg, 1987) suggesting a stepwise and uniform retreat across the entire eastern ASE (Fig. 1). Jakobsson *et al.* (2012) also described a series of regular 1–2 m-high corrugated ridges seaward of GZW3 associated with and transverse to curvilinear-linear furrows (Jakobsson *et al.*, 2011, 2012). The ridges have been interpreted as impressions resulting from the grounding of tidally-influenced icebergs that were calved directly from the GL during an ice shelf collapse from a GL position seaward of GZW3.

The timing of GL retreat is still poorly known, particularly on the outer and mid shelf areas. Kirshner *et al.* (2012) showed that glaciomarine sediments had started to accumulate seaward of GZW1 sometime before 16.4 cal. kyr BP (core PC07) and also argued that grounded ice had retreated seaward of GZW5 before 12.3 cal. kyr BP. The authors also speculated that this was followed by a second phase of ice shelf presence (12.3-10.6 cal. kyr BP; KC19) and break-up (KC23) (Kirshner *et al.* 2012). Inland of GZW5, Hillenbrand *et al.* (2013) demonstrated that inner Pine Island Bay (PIB) was free of grounded ice by 11.2 cal. kyr BP in core PS75/214-1 (NB: age recalibrated using MRE of  $1300 \pm 70$  years). Larter *et al.* (in press) has recently questioned whether the ages published in Kirshner *et al.* (2012) and Hillenbrand *et al.* (2013) are compatible as they would imply (i) very rapid retreat across the mid to inner shelf (i.e., between KC19 and PS75/214-1, Fig. 1); and (ii) a large ice shelf extending more than 200 km from the GL after its retreat into inner PIB. According to Larter *et al.* (in press) the apparent inability to accommodate the published chronological data with the geomorphological record could suggest that one of the age-datasets or facies interpretations is misleading. In addition, Graham *et al.* (2013) has also suggested that the corrugations may have been formed by other non-collapse bed-forming processes leaving room for an alternative deglaciation model for the eastern ASE. In light of these

uncertainties, new chronological data is required to improve our understanding of the glacial history of this rapidly changing area.

## 2. Method

Gravity cores (GC) and vibro-cores (VC) were recovered during expeditions JR141 and JR179 with RRS *James Clark Ross* and ANT-XXIII/4 and ANT-XXVI/3 with RV *Polarstern* to reconstruct the glacial history of the eastern ASE (Gohl, 2007; Larter *et al.*, 2007; Enderlein and Larter, 2008). Undisturbed seabed surface sediments were collected with (giant) box corers (GBC or BC). Core sites were focused along transect in the main PIT, PITE, Abbott and Cosgrove troughs (Fig. 1) with locations identified using an acoustic sub-bottom profiler. Physical properties (magnetic susceptibility, wet bulk density (WBD), and P-wave velocity) were measured on whole cores using GEOTEK multisensor core loggers (MSCL) at the British Ocean Sediment Core Research Facility (Southampton, UK) and at the Alfred Wegener Institute (AWI, Bremerhaven, Germany). The core sections were split at AWI and British Antarctic Survey (BAS) and shear strength was measured every 10-20 cm with a hand-held shear vane. Lithology, colour and sedimentary structures were described visually on the split cores and supplemented using smear-slides and x-radiographs. Individual sediment sub-samples (1 cm-thick slices) were then taken every 5-20 cm to determine contents of water, total carbon (TC), organic carbon ( $C_{org}$ ) and total nitrogen ( $N_{tot}$ ) and to analyse grain-size composition using techniques outlined in Smith *et al.* (2011). The relative contents of the clay minerals smectite, illite, chlorite and kaolinite were determined on an aliquot of the  $<2 \mu\text{m}$  fraction using standard X-ray diffraction methods described in Ehrmann *et al.* (2011). AMS  $^{14}\text{C}$  dating was carried out at the NERC Radiocarbon Laboratory (Environment) in East Kilbride (UK), and BETA Analytic Inc., Miami, Florida, U.S.A. (with prefix SUERC and BETA respectively in Table 1). Where possible  $\sim 10$  mg of calcareous microfossils were picked for dating under a microscope from the  $>63 \mu\text{m}$  fraction.  $^{14}\text{C}$  ages were calibrated with Calib v6.1.1, utilising the Marine09 calibration dataset (Reimer *et al.*, 2009) and a marine reservoir effect (MRE) correction of  $1300 \pm 70$  years (Berkman and Forman, 1996). Detailed lithological descriptions, photos and x-radiographs of the cores and all data published in this paper are available from the PANGAEA world data centre (<http://doi.pangaea.de/>) under <http://doi.pangaea.de/10.1594/PANGAEA.7549>.

### 2.1. Dating approach

Our dating strategy builds on the approach of Heroy and Anderson (2008) and Smith *et al.* (2011) who used detailed lithological description together with variations in physical

properties, grain-size, organic carbon and clay minerals to select the horizon in each core that would yield the most reliable AIO  $^{14}\text{C}$  deglacial age. The approach preferentially dates sediment from the open marine facies because it contains the least reworked fossil organic carbon while still representing the passing of the GL across the core site (Heroy and Anderson, 2008; Hillenbrand *et al.*, 2010a,b; Smith *et al.*, 2011). Consequently, the deglacial ages presented in this paper are 'minimum' ages for GL retreat.

### 3. Results and interpretation

#### 3.1. Lithological units and facies scheme

A total of 14 gravity/vibro-cores have been analysed (Table 1) with lithological units established on the basis of the core data. From this, three main facies have been identified which are described and interpreted below and illustrated in Figure 2 and supplementary Figure S1. The facies succession broadly follows that documented for sediments recovered in the western ASE (Smith *et al.*, 2009; 2011; Hillenbrand *et al.*, 2010b) and elsewhere on the Antarctic continental shelf (Domack *et al.*, 1999, 2005; Licht *et al.*, 1999; Evans *et al.*, 2005; Heroy and Anderson, 2005, 2007; Ó Cofaigh *et al.*, 2005; Hillenbrand *et al.*, 2005, 2010a,b, 2013; Pudsey *et al.*, 2006; Heroy *et al.*, 2008; McKay *et al.*, 2008) with a muddy diamicton at the base of the sequence, overlain by a transitional muddy sand/sandy-gravel which in turn is capped by a terrigenous to biogenic mud. The primary purpose of our facies approach is to establish the major depositional environments (subglacial, glacier proximal and open marine) to inform and direct our dating strategy.

#### *Facies 1a/b - Muddy diamicton*

The lowermost lithological unit in cores GC473, GC475, GC484, PS69/289-3, PS69/295-1, PS69/300-1, PS69/302-4 recovered a grey (typically 5Y 4/1 to 4/2 or 2.5Y 3/2) homogenous muddy diamicton, with shear strength values between 4-25 kPa, low water content and WBD, low  $C_{\text{org}}$  and high magnetic susceptibility. Angular to subrounded clasts are dispersed throughout in a muddy to sandy-muddy matrix. In general,  $\text{CaCO}_3$  is  $\leq 1.5$  wt.% but is higher in cores GC475, GC484 and PS69/295-1 reaching values  $\geq 1.5$  wt.%. Contacts with the overlying units are typically gradational, although sharp upper boundaries are observed in cores GC475, PS69/256-1 and PS69/302-4. The muddy diamictons were recovered from within the main PIT, or adjacent palaeo ice stream troughs (i.e., core PS69/300-1 in Cosgrove-Abbot Trough) in areas characterised by glacial lineations. Based on the absence of biogenic material in smear-slides, lack of sedimentological structures, low to moderate

shear strength and the fact that these sediments were recovered from areas of glacial lineations, we interpret the muddy diamicton as a mobile traction layer of deforming subglacial till, deposited beneath an ice stream (Facies 1a). The slightly elevated  $\text{CaCO}_3$  contents in cores GC484, GC475 and PS69/295-1 suggest that the muddy diamicton is partly composed of recycled glaciomarine sediments although the absence of glaciomarine sedimentary units within the diamicton indicates a single phase of glacier advance. Outer shelf cores PS69/302-4 and VC453 were recovered from areas of iceberg ploughmarks so we cannot completely rule out that the diamicton is an iceberg turbate, although in both instances shear strength increases gradually with depth which is more indicative of deformation tills rather than iceberg turbates. The latter often display more variable ('spiky') shear strength values (e.g., VC436, VC430 in Smith *et al.*, 2011).

A grey (5Y 4/1), homogenous, muddy diamicton was also observed at the base of PS69/256-1. PS69/256-1 was recovered from Abbot Trough at the toe of a large GZW (GZWa; see Fig. 1). Whilst displaying the sedimentological characteristics of a deformation till, the high sand content (>35 wt.%) together with its location at the toe of a wedge could suggest that the diamicton was deposited as a glaciogenic debris flows at or close to the GL rather than subglacially. Accordingly, we assign a sub-facies (Facies 1b) to this diamicton but note that the uncertainty over its genesis does not affect our interpretation of the deglacial age, which is taken from the base of the open marine unit.

#### *Facies 2 - Sandy-gravelly mud to muddy-gravelly sand*

Cores GC473, GC475, GC484, PS69/256-1, PS69/289-3, PS69/295-1, PS69/298-1 and PS69/300-1 contain a grey (typically 5Y 4/1 to 2.5 Y 4/2) crudely-stratified to structureless sandy-gravelly mud to muddy-gravelly sand with occasional sub-rounded to sub-angular pebbles. The unit is 7.5 to 209 cm thick and represents a transition between the muddy diamicton below and bioturbated mud above. Typically the transitional unit is characterised by an up-core decrease in shear strength, water content and WBD although trends do vary.  $C_{\text{org}}$  and  $\text{CaCO}_3$  values generally increase up-core although  $\text{CaCO}_3$  decreases in cores GC473, GC475 and PS69/298-1. Traces of diatoms and sponge spicules are present in the transitional unit of core PS69/302-4 and within the upper part of this unit at site GC473. The coarse-grained texture, low biogenic content and shear strength of the sandy-gravelly mud to muddy-gravelly sand unit together with its position above the diamicton indicates its deposition in close proximity to the GL during the transition from subglacial to glaciomarine conditions (sub-ice shelf or distal to the GL). However, the measured parameters do exhibit significant down-core variability, which is likely to reflect a setting proximal to distal from the

grounding line under an ice shelf, sea-ice or in open water. For example, at site GC475 the lower part of the transitional unit contains lower water and  $C_{org}$  contents, an absence of diatoms and a low gravel content compared to the upper part. We assign this lower part of the transitional unit to a GL proximal sub-ice shelf setting (Facies 2a) and suggest that the increase in gravel content within the upper part of the unit reflects the landward passing of the ice shelf calving front over the core site (Facies 2b) (c.f. Domack *et al.*, 1999). However, this is the only core where the distinction between sub-ice shelf and seasonal open marine conditions can be made and we cannot rule out that the transitional unit in other cores (e.g., PS69/295-1) was partly or wholly deposited beneath an ice shelf or perennial sea-ice coverage.

### *Facies 3- Mud*

The uppermost lithological unit in all cores consists of an olive brown (typically 2.5Y 4/4 to 10YR 4/3) mud with low concentrations of gravel and low shear strength ( $\leq 5$  kPa). The unit ranges in thickness from 17 to 912 cm and is generally characterised by an up-core decrease in grain-size, WBD and magnetic susceptibility and an increase in  $C_{org}$ .  $CaCO_3$  decreases up-core in cores GC473, GC475, GC484, PS69/289-3, PS69/295-1 and increases in cores VC453, GC479, PS69/256-1, PS69/298-1, PS69/300-1, PS69/302-4. In cores VC453 and PS69/256-1 the mud unit is bioturbated throughout and bears foraminifera in the upper c.16.5 and 13.5 cmbsf, respectively, while traces of diatoms and sponge spicules are present below these depths. In cores GC473, GC484, GC475, GC479 the mud unit is moderately bioturbated and bears diatoms in the upper c. 5 cm, whereas diatom content is  $<5\%$  further down-core. In core PS69/289-3 the mud is strongly bioturbated between c.16-211 cmbsf, slightly bioturbated between c.211 and 327 cmbsf and intermittently bioturbated between 327-336 cmbsf and 408-527 cmbsf. PS69/288-3 is moderately to slightly bioturbated between 36-215 cmbsf. X-radiographs show that the mud unit in core PS69/289-3 is moderately to strongly laminated between c. 146-256 cmbsf and slightly laminated throughout core PS69/295-1 and moderately laminated between 362-412 and 460.5-473 cmbsf in core PS69/288-3. Based on these observations we interpret the mud unit as a distal glaciomarine facies deposited primarily in a seasonally open marine environment. The dispersed gravel is interpreted as ice-rafted debris (IRD). The variable bioturbation throughout Facies 1, particularly in core PS69/298-3, could reflect periods of more persistent sea-ice conditions on the inner shelf, which limited productivity, although we cannot exclude the possibility that part of the unit was deposited beneath an ice shelf. More generally, the mud unit is thickest near the modern GL, which is likely to reflect their proximity to the sediment source over an extended period of time and is consistent with

previous studies from this area (Lowe and Anderson, 2002; Kirshner *et al.*, 2012; Hillenbrand *et al.*, 2013).

### 3.2. AMS $^{14}\text{C}$ chronology

We dated 69 samples; 18 surface sediment samples from GBCs and BCs (including one replicate AIO date), and 51 core-top and down-core samples from GCs and VCs (Table 2). Six seafloor surface and three down-core dates were obtained from calcareous microfossils (mainly planktonic and benthic foraminifera) and the rest on the AIO fraction primarily from Facies 3 (Table 2). We corrected all down-core AIO  $^{14}\text{C}$  dates by subtracting the seabed surface age of a box core recovered from the same or a nearby site (Licht *et al.*, 1999; Andrews *et al.*, 1999). Where a box core was unavailable, or its surface sample did not contain sufficient organic material for dating, we corrected the down-core dates by subtracting the core-top age of the VC/GC (e.g., cores PS69/295-1, PS69/298-1, PS69/300-1; Table 2). This approach is supported by data from core VC453, which yielded the oldest AIO  $^{14}\text{C}$  surface age in the study area but also yielded enough carbonate in a down-core horizon to allow paired AIO-foraminifera dating (Table 2). Calibrated ages are  $3865 \pm 107$  cal. yr BP on AIO (13 cmbsf) and  $4470 \pm 110$  cal. yr BP on foraminifera (14.5 cmbsf). Taking into account the analytical uncertainty as well as the low sedimentation rates on the outer shelf, these ages are remarkably consistent and provide further support for our AIO-based dating approach.

#### *Seafloor surface and core-top ages*

Ages on calcareous microfossils range from 2653 to 1144  $^{14}\text{C}$  yr BP whilst AIO dates yielded significantly older ages (10,667 to 3477  $^{14}\text{C}$  yr BP) reflecting the variable input of reworked fossil organic carbon (Table 2). Two systematic trends in the AIO surface and core-top ages are apparent: (1) the eastern coastline is characterised by comparatively 'young' ages (3618-2285  $^{14}\text{C}$  yr BP); and (2) the main Pine Island Trough is characterised by comparatively 'old' ages (6018-10667  $^{14}\text{C}$  yr BP) (Fig. 3). This pattern indicates differences in the flux of reworked fossil organic carbon from the catchment which is in agreement with the mapped clay mineral provenance data (Ehrmann *et al.*, 2011). Ehrmann *et al.* (2011) showed that the highest concentrations of kaolinite occur north of Thwaites Glacier whilst the lowest values are found near the Cosgrove Ice Shelf. Kaolinite indicates the presence of pre-Oligocene sedimentary strata in the hinterland (or sediments containing recycled pre-Oligocene detritus) and potentially provides a proxy for the input of reworked fossil organic carbon because such sedimentary strata are often enriched in organic matter. In the eastern

ASE the most likely source of kaolinite lies in the Byrd Subglacial Basin which has an estimated infill of c. 500 m of unconsolidated sediments of unknown composition and age (Winberry and Anandakrishnan 2004, Bell *et al.*, 2006, LeMasurier 2008). The Thwaites Glacier catchment provides a direct connection to the Byrd Subglacial Basin and thus an obvious pathway for detritus derived from fossil-carbon-bearing sedimentary rocks. In contrast there is no obvious kaolinite source in NW Ellsworth Land which could explain the younger  $^{14}\text{C}$  ages along the easternmost ASE (Fig. 4).

#### *Down-core $^{14}\text{C}$ ages and bulk organic and clay mineral parameters*

Down-core AIO  $^{14}\text{C}$  ages range from 4380 to 41,657  $^{14}\text{C}$  yr BP (Table 2) with age reversals observed in cores VC453, GC479, PS69/256-1 and PS69/289-1 (Fig. 2 and Fig. S1). Systematic trends in the down-core data are also apparent, which are likely to reflect spatial variability in the input of fossil carbon. Postglacial sediments in cores from the mid-outer shelf produced consistently 'old' ages whilst those from Cosgrove-Abbott are generally 'younger'. These 'old'  $^{14}\text{C}$  ages, which are particularly apparent in the transitional sediments (Facies 2) of several cores (uncorrected  $^{14}\text{C}$  dates  $\geq 30$  kyr BP e.g., GC473, GC484, PS69/256-1) reflects the admixture of high amounts of fossil organic carbon, confirmed by the discovery of a large coal fragment in subglacial till in core PS75/235-2 (see Pangaea link: <http://doi.pangaea.de/10.1594/PANGAEA.754982>).

We also explored the possibility of using bulk organic (C/N,  $\delta^{13}\text{C}$ ) and clay mineral parameters to assess the reliability of the down-core age data (e.g., Hillenbrand *et al.*, 2010a) but found no significant correlations (Fig. S2). However, whilst it is not possible to derive a 'reliability threshold' for AIO ages using these parameters, C/N and kaolinite values are nevertheless useful when assessing broad-scale patterns in the input of fossil carbon i.e., samples with 'old' ages are typically characterised by high kaolinite and high C/N values (Fig. S2).

#### *Deglacial ages for the eastern ASE*

The following section establishes a deglacial framework for the eastern ASE and we explain the specific factors for omitting ages from our model. On the outer shelf, the base of Facies 3 in core PS69/302-4 was dated to 12.9 cal. kyr BP (Fig. S1i and Fig. 5) which is considerably younger than nearby core PC07 (i.e., 16.4 cal. kyr BP recalibrated from Kirshner *et al.*, 2012). Thus it is likely that PS69/302-4 has been subject to winnowing or erosion by currents and icebergs, respectively and is not included in our model (Fig. 5). The

most reliable constraint on deglaciation of the outer shelf is provided by core VC453. Age reversals from within the two sandy mud beds (Fig. 2b) indicate sediment reworking, likely by current winnowing or debris flows, and are omitted from our deglacial chronology. The remaining three ages are in stratigraphic order, with the lowermost date directly above Facies 1 yielding a minimum deglacial age of 20.6 cal. kyr BP. Inland of VC453,  $^{14}\text{C}$  ages from Facies 2 and 3 in core GC473 display a prominent dog-leg between 16 and 18.5 cmbsf whilst the lowermost  $^{14}\text{C}$  age is radiocarbon dead (Fig. S1a). Consequently we dismiss all of these ages from our deglacial chronology. Core PS69/256-1, located in the Abbot Trough, yielded an age of 15.7 cal. kyr BP for the base of Facies 3 (Fig. 2a, Table 2). An older age of 18.0 cal. kyr BP was obtained from a horizon directly above this sample resulting in an upper and lower estimate for the minimum age for deglaciation.  $^{14}\text{C}$  ages from Facies 2 and 3 at site GC484 on the mid-shelf also display a significant dog-leg and are not included in our deglacial framework (Fig. S1c). GC484 was recovered from an area of oceanward dipping sedimentary strata, estimated to be Late Cretaceous to Mid-Miocene in age, which crop out close to the sea-floor (Gohl *et al.*, 2013). The dated sediments are also characterised by high kaolinite contents (Fig. S2a), suggesting that these dipping strata represent a major source of fossil organic carbon and that their subglacial “recycling” is responsible for the anomalously old AIO ages in this area (e.g., GC484, GC473 and also ages from Klages *et al.* (2013) discussed below). Further landward,  $^{14}\text{C}$  ages from GC475 (within the GL-proximal part of Facies 2) constrain retreat of grounded ice to sometime prior to 10.1 cal. kyr BP (Fig. 2c). Cores PS69/300-1 and PS69/298-1 were recovered to the east of the main PIT and constrain GL-retreat on this part of the shelf to 13.6 cal. kyr BP and 13.2 cal. kyr BP, respectively (Fig. 5). We omit the lowermost age in core PS69/300-1 because it occurs within a  $^{14}\text{C}$  dog-leg (Fig. S1h). Indeed the contact between Facies 2 and 3 is characterised by higher kaolinite values suggesting proportionally more input of reworked fossil organic matter in the lowermost transitional sediments (see Pangaea link xx). On the inner shelf, core GC479 recovered only Facies 3, dated to between 10.1-13.1 cal. kyr BP (Fig. S1b). The  $^{14}\text{C}$  ages obtained from Facies 3 in core PS69/295-1 constrain retreat of grounded ice to 10.6 cal. kyr BP (Fig. S1g) with the two lowermost ages from this core forming a significant  $^{14}\text{C}$  dog-leg that is also reflected in the high kaolinite values. Finally ages from Facies 3 in core PS69/289-3 (14.8-25.9 cal. kyr BP; Fig. 2f) are not included in our deglacial chronology because they are considerably older than both the timing of deglaciation inferred from mid-shelf cores (Fig. 5a), as well as previously published  $^{14}\text{C}$  dates on calcareous microfossils from the inner shelf (c. 11.6-9.2 cal. kyr BP; Hillenbrand *et al.*, 2013).

#### 4. Discussion

#### 4.1. New constraints on the timing of grounded ice retreat in the eastern ASE

In the following section we discuss the new deglacial data from the outer, mid and inner shelf along a single latitudinal transect (see Fig. 1). This reflects the apparent continuity of GZWs mapped in both the PITE and Abbot Trough and the PIT and Cosgrove Trough (Fig. 1) (Graham *et al.*, 2010; Jakobsson *et al.*, 2012; Klages, 2014). With the exception of several clear outliers (PS69/302-4, GC484, GC475, PS69/289-3) the new dataset shows a consistent pattern of deglaciation across the eastern ASE shelf (Fig. 5) and indicates that grounded ice had retreated from the outer shelf by 20.6 cal. kyr BP (core VC453), and to the latitude of GZW1 by 15.7-18.0 cal. kyr BP (core PS69/256-1; Fig. 1 and Fig. 5). Deglaciation of the mid-shelf area, particularly in PIT, remains poorly constrained due to insufficient core coverage as well as problems affecting the AIO  $^{14}\text{C}$  dating of the sediments in this area. This issue is most clearly highlighted by the down-core AIO  $^{14}\text{C}$  ages from cores GC473 and GC484 (Fig. 5a) which are much older than the regional deglaciation and indicate a significant input of recycled fossil organic carbon which is probably sourced from the underlying sedimentary strata (see Gohl *et al.*, 2013; Klages, 2014). In contrast, sediments cored in Cosgrove Trough appear to be least affected by input of reworked fossil organic carbon, and indicate GL retreat before 13.2-13.6 cal. kyr BP (Fig. 5). Since GZWs mapped in Cosgrove Trough are thought to be continuations of the GZWs in PIT (Klages, 2014), the ages from Cosgrove Trough can be used to infer the relative timing of GL retreat in the main trough and vice versa. Core GC475 (located just landward of GZW5) reveals that glaciomarine sedimentation was underway sometime prior to 10.1 cal. kyr BP in the main PIT (Fig. 5a), but this age is significantly younger than the deglaciation age of 13.6 cal. kyr BP obtained from core PS69/300-1 in Cosgrove Trough (located just landward of GZWb) and is also younger than a foraminifera-based deglacial age from inner Pine Island Bay (Hillenbrand *et al.* 2013). We suggest that the deglacial age from core GC475 represents retreat of the calving margin of an ice shelf rather than grounded ice retreat (discussed further below). Further inland of GZW5, cores GC479 and PS69/295-1 record a consistent GL retreat over the inner shelf to within c.150 km of the PIG ice shelf front before 10.6 cal. kyr BP.

#### 4.2. Deglaciation of the eastern ASE – a regional framework

Our new chronological data is largely consistent with previously published deglacial ages from the eastern ASE (e.g., Kirshner *et al.* 2012; Hillenbrand *et al.* 2013) (Fig. 6). Obvious exceptions to this are the AIO ages from Klages *et al.* (2013) and the few  $^{14}\text{C}$  ages on calcareous foraminifera published in Lowe and Anderson (2002). Klages *et al.* (2013) dated

AIO samples of two cores to the east of PIT which suggested that the deglaciation occurred between 19.2 cal. kyr BP and 17.7 cal. kyr BP. Whilst the ages are not wholly inconsistent with the timing of deglaciation of the outer shelf (see Fig. 6) it seems most likely that these 'older' ages reflect a greater degree of contamination with reworked fossil organic carbon, and much like the down-core ages from GC484 and GC473, are considered to be unreliable. A low reliability has previously been assigned to the deglacial age from PC39 ( $17.4 \pm 9.4$  cal. kyr BP; Lowe and Anderson 2002), located to the west of Burke Island owing to the small sample size of the dated material (e.g., Larter *et al.*, in press).

Deglaciation of the PITE trough commenced sometime before 20.6 cal. kyr BP, c. 4200 earlier than the minimum deglacial age of the outer shelf documented in Kirshner *et al.* (2012) (core PC07) but consistent with the onset of deglaciation in the western ASE (Fig. 6) (22.3 cal. yr BP; Smith *et al.*, 2011). Landward of VC453, geomorphological data reveal a complex pattern of retreat punctuated by a series of prolonged still-stands in both PIT and Abbot-Cosgrove Trough (GZW's 1-5,a & b marked on Figure 1), one (Jakobsson *et al.*, 2011) or possibly two phases of ice shelf break-up (Kirshner *et al.*, 2012) as well as a readvance (Jakobsson *et al.*, 2012). A readvance is also documented on the inter-ice stream ridge separating the two troughs (Klages *et al.*, 2013). However, because of the difficulties in dating sediments in this area the style and timing of retreat is reliant on interpretation of the geomorphological record, which is also unclear (cf. Kirshner *et al.*, 2012; Jakobsson *et al.*, 2012). For instance, corrugation ridges to the north of GZW3 have been taken to indicate a 'first' phase of ice shelf break-up, as the grounding line retreated landward to GZW4 (Jakobsson *et al.*, 2011, 2012). Deposition of GZW4 has been associated with ice-stream readvance, but this is poorly constrained occurring sometime before 12.3 cal. kyr BP (Jakobsson *et al.*, 2012). From its location at GZW4 the ice sheet is then thought to have stepped back to GZW5 where, the GL was elevated to between 726-670m as the wedge developed (Jakobsson *et al.* 2012). Kirshner *et al.* (2012) have provided the only age-constraint on these changes, indicating that ice had retreated landward of GZW5 sometime before 12.3 cal. kyr BP. The authors also argued that the mid-shelf was again covered by a large ice shelf between 12.3 and 10.6 cal. kyr BP with the GL positioned somewhere on the inner shelf. Sedimentological changes at the end of this interval (Kirshner *et al.*, 2012) and corrugation ridges within or overprinting MSGL on top of GZW4 (Jakobsson *et al.*, 2012) have been interpreted as indicating a 'second' phase of ice shelf break-up and rapid grounding line retreat into inner PIB after 10.6 cal. kyr BP. More recently Hillenbrand *et al.* (2013) demonstrated that the GL had already retreated into inner PIB by 11.2 cal. kyr BP which is also supported by the AIO ages presented in this study (Fig. 6).

Larter *et al.* (in press) raised the issue that, if the Kirshner *et al.* (2012) and Hillenbrand *et al.* (2013) datasets were both correct, they would imply rapid retreat across the middle to inner shelf (Fig. 7a, Trajectory B), with a large ice shelf extending more than 200 km from the GL after it had retreated into inner PIB. Whilst both scenarios are possible, the description of 'glacier-proximal' sediments to the north of GZW3 (Fig. 1) (subunit 2-A in core KC06) dated to between 8.2 to 10.8 cal. yr BP (Fig. 6) does raise questions about the deglacial model published in Kirshner *et al.* (2012). Furthermore, if the Jakobsson *et al.* (2011) model for formation of corrugations is also correct, then the ridges imaged on GZW4 must have formed before GZW5, otherwise it would have been impossible to generate icebergs with deep enough keels to form them (see Fig. 4 in Jakobsson *et al.*, 2012). It follows therefore that GZW5 must have formed after ice shelf break-up, but this appears to be in conflict with rapid GL retreat onto the inner shelf implied by the 11.2 cal. kyr BP age in Hillenbrand *et al.* (2013).

One alternative scenario offered by our new dates is that the GL had retreated from the mid-shelf earlier than previously thought. The apparent continuity of GZWs in both the PITE and Abbot Trough and the main PIT and Cosgrove Trough (Klages, 2014) suggests that the ice margin stepped back uniformly. Using this model, and the ages from the Cosgrove Trough, the mid-shelf was free of grounded ice at least 1000 years earlier than suggested by Kirshner *et al.* (2012) (13.6 rather than 12.3 cal. kyr BP). This scenario would help accommodate the time required to form GZW5 (estimated to have taken 600-2000 years; Jakobsson *et al.* 2012) and subsequent retreat of the grounding line onto the inner shelf by 11.2 cal. kyr BP.

Assessing whether an ice shelf covered the ASE during the post-LGM deglaciation is also complex since no single diagnostic proxy for ice shelf cover exists. The presence of pelletized mud, a sediment composition indicating low biological productivity, low content of IRD that has a specific provenance, fine-grain size and lamination or stratification of sediments as well as specific benthic foraminiferal assemblages have all been used to reconstruct ice shelf presence (e.g. Powell 1994; Domack and Harris, 1998; Domack *et al.*, 2005; Licht *et al.*, 1999; Pudsey and Evans, 2001; Hemer and Harris, 2003; Pudsey *et al.*, 2006; Hemer *et al.*, 2007; McKay *et al.* 2008; Jakobsson *et al.*, 2010; Polyak and Jakobsson, 2011). Palaeo-studies using multiple lines of evidence offer the most robust approach (e.g., Smith *et al.*, 2007; Kilfeather *et al.*, 2011) but even this strategy is complicated by results from beneath modern ice shelves which show that open marine indicators (diatoms and planktic foraminifera) are advected up to 100 km underneath them and sustain a diverse benthic fauna assemblage also typical for open-marine settings (Hemer and Harris, 2003;

Domack *et al.*, 2005; Hemer *et al.*, 2007; Riddle *et al.*, 2007; Post *et al.* 2014). In the eastern ASE, Kirshner *et al.* (2012) described a 'sub-ice shelf' facies in just two cores from the mid-shelf part of PIT (Unit 3 in cores KC19 and KC25 which were 27 cm and 2.5 cm thick, respectively) and also speculated that an ice shelf extended across the entire ASE. Their interpretation of an ice shelf in the eastern ASE was based principally on the low abundance of IRD and occurrence of planktonic foraminifera (*N. pachyderma* sin.). *N. pachyderma* sin. have been previously documented in sub-ice shelf sediments deposited beneath the Larsen B and Amery ice shelves (Domack *et al.*, 2005; Hemer *et al.*, 2007) but are more commonly found in open-marine settings elsewhere on the Antarctic shelf (e.g. Hauck *et al.*, 2012) so cannot be used as an indicator for ice shelf presence. Facies 2a in core GC475 from the mid-shelf has characteristics similar to the sub-ice shelf facies reported by Kirshner *et al.* (2012), but is coarser-grained. The diatom-barren terrigenous sandy mud bears only a few scattered larger clasts and gravel grains, has low  $C_{org}$  content and is therefore a candidate for deposition beneath an ice shelf. The increase of coarser material within overlying Facies 2b, dated to 10.1 cal. kyr BP, could reflect the retreat of the ice-shelf's calving line from the core site (e.g., Domack *et al.*, 1999). If correct, this would lend support to the idea that an ice shelf existed on the mid-shelf until c. 10 cal. kyr BP. The existence of an ice shelf in PIB may also help explain the apparent lag in the timing of inland thinning of PIG during the early Holocene. Dating rock erratics in the Hudson Mountains (Fig. 1) Johnson *et al.* (2014) documented a period of rapid and sustained thinning of PIG around 8 kyrs BP, several thousand years after the GL had retreat to the inner shelf (i.e., 11.2 cal. kyr BP). Because there are no topographic highs landward of where the GL might have been pinned after 11.2 cal. kyr BP, they speculated that the lag may have been caused by an extensive ice shelf in PIB that buttressed inland ice after the GL had retreated. If correct this would imply that the ice shelf calving margin retreated landward of GC475 after 10.1 cal. kyr but persisted in PIB until c. 8 cal. kyr BP. Unfortunately there are no dated cores landward of core PS75/167-1 to constrain the GL position and, as discussed above, the available sedimentological evidence for ice shelf presence/absence in PIB is inconclusive.

Kirshner *et al.* (2012) also suggested that the ice shelf extended over the western ASE (see their Fig. 8) based on the apparent similarity of fine-grained sediment facies in core KC19 (interpreted as 'sub-ice shelf' facies by Kirshner *et al.*, 2012) and core VC419, which was recovered north of the Dotson Ice Shelf (Smith *et al.*, 2009). We point out that it is not supported by the published interpretation of sediment facies in the area (cf. Smith *et al.*, 2011) and remains speculative. For instance, well-preserved diatomaceous ooze layers in cores recovered in the Dotson-Getz Trough indicate deglaciation by 12.6 cal. kyr BP (Hillenbrand *et al.*, 2010b). Whilst the deposition of diatom-bearing sediments beneath an ice

shelf cannot be completely ruled out (cf. Hemer and Harris, 2003), the high abundance and pristine preservation of the diatoms in the sediments from the Dotson-Getz Trough indicates that highly productive marine conditions existed on the inner western ASE shelf during the proposed interval of ice shelf presence in the eastern ASE (cf. Kirshner *et al.*, 2012).

Finally, in addition to these sedimentological considerations, recent work has shown that the corrugation ridges described by Jakobsson *et al.* (2011, 2012), could reflect another bed shaping process. Graham *et al.* (2013) described corrugations and ploughmarks on a ridge beneath the modern PIG ice shelf and suggested their formation by periodic grounding of ice shelf keels during glacier unpinning rather than ‘catastrophic’ ice shelf collapse. Therefore, and in summary, the presence of a large fringing ice shelf over the mid-inner shelf of the eastern ASE is still open to debate and requires additional, multi-proxy work to confirm or dismiss this scenario. The new deglacial data presented in this study indicates that the GL retreated from the mid-shelf earlier than 12.6 cal. yr BP which would help accommodate both the formation of GZW5 and the rapid retreat to the inner shelf implied by the ages in Hillenbrand *et al.* (2013) (Table 3).

#### 4.3. What can we say about the trajectory of deglaciation in the Amundsen Sea?

The past decade has witnessed a significant improvement in our understanding of the former extent and flow of the WAIS in the ASE (e.g., Larter *et al.*, 2007; in press; Graham *et al.*, 2009; 2010; 2013; Smith *et al.*, 2009; 2011; Hillenbrand *et al.*, 2010b; 2013; Jakobsson *et al.*, 2011; 2012; Kirshner *et al.*, 2012; Klages *et al.*, 2013). This has been used to build a picture of GL retreat in the Amundsen Sea sector of WAIS since the LGM (Larter *et al.*, in press), which is needed to constrain ice sheet and glacial-isostatic adjustment models (Bentley *et al.* in press). Our new chronological data from the eastern ASE contributes to this effort and shows that the GL had retreated from the shelf edge by 20.6 cal. kyr BP, reached the mid-shelf between 13.6 to 12.6 cal. kyr BP and the inner shelf, to within c.110 km of the modern GL, as early as 11.2 cal. kyr BP (Fig. 6). The lack of clear evidence for a significant GL readvance after 11.2 cal. kyr BP could suggest these changes were followed by a period of relative stability (e.g., Hillenbrand *et al.*, 2013) although core information and chronological data from the inner shelf, especially beneath the ice shelf and near the modern GL are still sparse (e.g. Nitsche *et al.*, 2013). In addition, recent surface exposure dating in the hinterland indicates that PIG underwent a period of rapid thinning in the early Holocene. This could imply the GL was more dynamic during the Holocene although the apparent lag between inland thinning and GL retreat to the inner shelf by c.11.2 cal. yr BP might also

suggests that inland ice was insensitive to changes in the position of the GL, perhaps because of an ice shelf in PIB.

In general terms, the timing and 'trajectory' of ice sheet retreat in the eastern ASE is similar to that observed in Dotson-Getz Trough (Fig. 6), which shows a slow GL retreat across the outer shelf, more rapid GL retreat over the middle to inner shelf followed by very slow retreat throughout the Holocene (see Fig. 8 in Smith *et al.* 2011). Here Smith *et al.* (2011) attributed the rapid retreat across the mid-inner shelf to the landward-increasing reverse gradient and a similar relationship is apparent in PIT (Fig. 7). However, while the affect of topography is evident in both deglacial scenarios (Trajectory A & B; Fig. 7) we cannot definitively say which of the two scenarios is correct. Our favoured scenario (trajectory A) critically depends on the time taken to deposit GZW5 as only very rapid deposition, and probably at the lower end of the 600-2000 years estimated by Jakobsson *et al.* (2012), would result in trajectory B. There are of course numerous other 'deglacial trajectories' through the available data, some resulting in even more rapid retreat across the deeper inner shelf which highlights the need for more data as well as modelling (cf. Jamieson *et al.*, 2014). It is also likely that other factors (e.g., incursion of CDW, phases of rapid sea-level rise) played a major role in driving the deglaciation (cf. Smith *et al.* 2011) but their relative importance, phasing and the persistence of these forcings through the deglaciation need to be investigated using more sophisticated proxy-based work and also modelling.

Thus, although the available datasets and chronologies (Fig. 6 and Table 3) reveal a broadly consistent pattern of deglaciation (i.e., slow-fast-slow) and capture some complexity of ice-stream dynamics (e.g., more rapid GL retreat across deep inner shelf basins; Fig. 7), much of the detail, such as the duration of still-stands/pauses or re-advances during deglaciation, remain unresolved. Deglaciation of the middle shelf, particularly in the main PIT, remains poorly constrained although new data from Cosgrove Trough may suggest that it occurred earlier than previously thought, which would favour an 'A' style retreat trajectory. Questions also remain about the possible extent and retreat history of ice shelves and the signature of these events in the sedimentary and geomorphological record, which ultimately requires further work on modern sub-ice shelf settings and sediments. However, the biggest limiting factor in deciphering these changes is our ability to date them. As several authors have pointed out,  $^{14}\text{C}$  dating of calcareous (micro-)fossils is preferable but this is not always possible and can also result in significant down-core age reversal (see  $^{14}\text{C}$  dates for cores VC436 in Smith *et al.*, 2011, and PS75/160-1 in Hillenbrand *et al.*, 2013). Our study demonstrates that even in the absence of the 'holy-trinity' of LGM to Holocene sediments on the Antarctic continental shelf (three-fold sediment sequence consisting of subglacial,

transitional and open-marine facies, the presence of carbonate directly above the sub-glacial contact, carbonate ages in stratigraphic order) deglacial frameworks can be established through careful inspection of large AIO datasets. In this context, future work in the ASE should place a greater emphasis on (i) constraining the timing of grounding line still-stands, (ii) providing clear evidence for possible phases of GL re-advance, and (iii) reconstructing former ice-shelf extent both spatially and temporally. For outer shelf areas a greater coverage of cores is required with a concerted effort to target areas that are not heavily scoured by icebergs. For the inner shelf, which is mainly formed of bedrock with only very localised sediment coverage (e.g. Lowe and Anderson, 2003; Graham *et al.*, 2009; Nitsche *et al.*, 2013), closer inspection of sub-bottom acoustic data is required to help locate shallow pockets of sediment that have the potential to bear high abundances of calcareous (micro-)fossils (e.g., Hillenbrand *et al.*, 2013) and that are ideally unaffected by iceberg scouring. This is especially needed for the inner shelf areas directly in front of the modern calving margin and beneath the ice shelf where the GL history is unknown. Finally more detailed analyses of sedimentological and chronological data is required to tie the complex geomorphological record to the sedimentary sequences.

## 5. Conclusion

- New sedimentological and chronological data from the eastern ASE indicates that grounding-line retreat from the outer shelf began before 20.6 cal. kyr BP with retreat to the mid-shelf occurring as early as 13.6 cal. yr BP (Fig. 5b). Two cores recovered from the inner shelf indicate that the grounding line had retreated to within 150 km of its current position by 10.6 cal. yr BP. In combination with geomorphological data showing that GZWs occur in different troughs at similar latitudes, the new dataset suggests that the ice sheet margin retreated uniformly across the eastern ASE.
- Our deglacial model is broadly consistent with previously published ages although our new dates suggest that ice retreated from the outer and middle shelf areas earlier than previously thought (Table 3). An earlier retreat on the mid-shelf could help reconcile the datasets of Kirshner *et al.* (2012) and Hillenbrand *et al.* (2013).
- The timing and 'trajectory' of GL retreat in the eastern ASE is consistent with that observed in the western ASE showing slow retreat across the outer shelf and faster retreat from the middle to inner shelf (Fig. 6, Table 3). This suggests a common forcing across the entire ASE. However, whilst the importance of a reverse bedslope

is apparent in both the western and eastern datasets the relative contribution of and interplay between the various drivers (i.e., CDW upwelling, sea-level rise and shelf topography) can only be disentangled by more detailed multi-proxy work as well as palaeo-ice stream modelling.

- Finally, despite an increase in chronological data from the ASE over the last few years documenting the LGM to Holocene glacial history it remains difficult to resolve “small scale” changes, such as the duration of grounding line still-stands and possible readvances. This clearly highlights the need for additional marine geological data from the area in order to better constrain ice sheet models and to investigate the mechanisms responsible for forcing ice sheet retreat.

## 6. Acknowledgements

This study is part of the British Antarctic Survey ‘Polar Science for Planet Earth Programme (Palaeo-Ice Sheets work package)’, funded by The Natural Environment Research Council. Additional funding from the Alfred Wegener Institute research programme Polar Regions and Coasts in a Changing Earth System, the UK Natural Environment Research Council (NERC) New Investigator Grant NE/F000359/1 and the Deutsche Forschungsgemeinschaft (grant to Werner Ehrmann) is also acknowledged. We also wish to thank the expert technical help of Jeremy Sothcott (BOSCORF) for help with core logging as well as NDT-Intertek services (Simon Taylor and Robert Collington) for providing core x-rays. In addition, we thank the captains, officers, crew, support staff and scientists who participated in cruises JR141, JR179 and ANTXXIII/4 and laboratory support from Hilary Blagbrough at BAS.

## 7. References

Andrews, J.T., Domack, E.W., Cunningham, W.L., Leventer, A., Licht, K.J., Jull, A.J.T., DeMaster, D.J., Jennings, A.E., 1999. Problems and possible solutions concerning radiocarbon dating of surface marine sediments, Ross Sea, Antarctica. *Quaternary Research* 52, 206–216.

Bell, R.E., Studinger, M., Karner, G., Finn, C.A. Blankenship, D.A., 2006. Identifying major sedimentary basins beneath the West Antarctic Ice Sheet from aeromagnetic data analysis. In Fütterer, D.K., Damaske, D., Kleinschmidt, G., Miller, H., Tessensohn, F., eds. *Antarctica: contributions to global earth sciences*. Berlin: Springer, 117–121.

Bentley, M.J., 2009. The Antarctic palaeo record and its role in improving predictions of future Antarctic Ice Sheet change. *Journal of Quaternary Science* 25, 5-18.

Bentley, M.J. and 77 others. In press. A community-based reconstruction of Antarctic Ice Sheet deglaciation since the Last Glacial Maximum. *Quaternary Science Reviews* 10.1016/j.quascirev.2014.06.025.

Berkman, P.A., Forman, S.L., 1996. Pre-bomb radiocarbon and the reservoir correction for calcareous marine species in the Southern Ocean. *Geophysical Research Letters* 23, 363-366.

Domack, E.W., Jacobsen, E.A., Shipp, S.S., Anderson, J.B., 1999. Late Pleistocene – Holocene retreat of the West Antarctic ice sheet system in the Ross Sea: a new perspective: Part 2, Sedimentologic and stratigraphic signature. *Geological Society of America Bulletin* 111, 1517– 1536.

Domack, E., Duran, D., Leventer, A., Ishman, S., Doane, S., McCallum, S., Amblas, D., Ring, J., Gilbert, R., Prentice, M., 2005. Stability of the Larsen B ice shelf on the Antarctic Peninsula during the Holocene epoch. *Nature* 436, 681-685.

Domack, E.W., Harris, P.T., 1998. A new depositional model for ice shelves, based upon sediment cores from the Ross Sea and the MacRobertson shelf, Antarctica. *Annals of Glaciology* 27, 281-284

Dowdeswell, J.A., Evans, J., Ó Cofaigh, C., Anderson, J.B., 2006. Morphology and sedimentary processes on the continental slope off Pine Island Bay, Amundsen Sea, West Antarctica. *Geological Society of America Bulletin* 118, 606-619.

Enderlein, P., Larter, R.D. (Eds.), 2008. Cruise Report JR 179, RRS James Clark Ross, February to April 2008, Marine biological and marine geological and geophysical studies in the Amundsen and Bellingshausen Seas: British Antarctic Survey, 167 pp., ([https://www.bodc.ac.uk/data/information\\_and\\_inventories/cruise\\_inventory/report/jr179.pdf](https://www.bodc.ac.uk/data/information_and_inventories/cruise_inventory/report/jr179.pdf)), Cambridge, UK.

Ehrmann, W., Hillenbrand, C.-D., Smith, J.A., Graham, A.G.C., Kuhn, G., Larter, R.D., 2011. Provenance changes between recent and glacial-time sediments in the Amundsen Sea embayment, West Antarctica: Clay mineral assemblage evidence. *Antarctic Science* 23, 471-486.

Evans, J., Dowdeswell, J.A., Ó Cofaigh, C., Benham, T.J., Anderson, J.B., 2006. Extent and dynamics of the West Antarctic Ice Sheet on the outer continental shelf of Pine Island Bay during the last glaciation. *Marine Geology* 230, 53-72.

Evans, J., Pudsey, C.J., 2002. Sedimentation associated with Antarctic Peninsula ice shelves: implications for palaeoenvironmental reconstructions of glaciomarine sediments. *Journal of the Geological Society* 159, 233-237.

Evans, J., Pudsey, C.J., Ó Cofaigh, C., Morris, P., Domack, E., 2005. Late Quaternary glacial history, flow dynamics and sedimentation along the eastern margin of the Antarctic Peninsula Ice Sheet. *Quaternary Science Reviews* 24, 741-774.

Fairbanks, R.G., Mortlock, R.A., Chiu, T-C., Cao, L., Kaplan, A., Guilderson, T.P., Fairbanks, T.W., Bloom, A.L., 2005. Marine Radiocarbon Calibration Curve Spanning 0 to 50,000 Years B.P. 2005. Based on Paired  $^{230}\text{Th}/^{234}\text{U}/^{238}\text{U}$  and  $^{14}\text{C}$  Dates on Pristine Corals. *Quaternary Science Reviews* 24, 1781-1796.

Favier, L., Durrand, G., Conford, S.L., Gudmundsson, G., Gagliardini, O; Gillet-Chaulet, F., Zwinger, T., Payne, A.J., Le Brocq, A.M. 2014. Retreat of Pine Island Glacier controlled by marine ice-sheet instability. *Nature Climate Change* 4, 117-121 doi:10.1038/nclimate2094.

Gladstone, R.M., Lee, V., Rougier, J., Payne, A.J., Hellmer, H., Le Brocq, A., Shepherd, A., Edwards, T.L., Gregory, J., Cornford, S.L. 2012. Calibrated prediction of Pine Island Glacier retreat during the 21<sup>st</sup> and 22<sup>nd</sup> centuries with a coupled flowline model. *Earth and Planetary Science Letters* 333–334, 191-199.

Gohl, K. (Ed.), 2007. The Expedition ANTARKTIS-XXIII/4 of the Research Vessel “Polarstern” in 2006. *Berichte zur Polar- und Meeresforschung (Reports on Polar and Marine Research)*, vol. 557. Alfred-Wegener- Institut für Polar- und Meeresforschung, Bremerhaven (Germany), 166 pp. <http://epic.awi.de/26756/>.

Gohl, K., Uenzelmann-Neben, G., Larter, R.D., Hillenbrand, C.-D., Hochmuth, K., Kalberg, T., Weigelt, E., Davy, B., Kuhn, G., Nitsche, F.O., 2013. Seismic stratigraphic record of the Amundsen Sea Embayment shelf from pre-glacial to recent times: evidence for a dynamic West Antarctic ice sheet. *Marine Geology* 344, 115-131.

Graham, A.G.C., Larter, R.D., Gohl, K., Hillenbrand, C.-D., Smith, J.A., Kuhn, G., 2009. Bedform signature of a West Antarctic palaeo-ice stream reveals a multi-temporal record of flow and substrate control. *Quaternary Science Reviews* 28, 2774-2793. doi:10.1016/j.quascirev.2009.07.003.

Graham, A.G.C., Larter, R.D., Gohl, K., Dowdeswell, J.A., Hillenbrand, C.-D., Smith, J.A., Evans, J., Kuhn, G., 2010. Flow and retreat of the Late Quaternary Pine Island-Thwaites palaeo-ice stream, West Antarctica. *Journal of Geophysical Research: Earth Surface* 115, F03025, doi:10.1029/2009JF001482.

Hauck, J., Gerdes, D., Hillenbrand, C.-D., Hoppema, M., Kuhn, G., Nehrke, G., Völker, C., and Wolf-Gladrow, D.A., 2012. Distribution and mineralogy of carbonate sediments on Antarctic shelves: *Journal of Marine Systems* 90, 77-87.

Hemer, M.A., Harris, P.T. 2003. Sediment core from beneath the Amery Ice Shelf, East Antarctica, suggests mid-Holocene ice-shelf retreat. *Geology* 31, 27-130.

Hemer, M.A., Post, A.L., O'Brien, P.E., Craven, M., Truswell, E.M., Roberts, D., Harris, P., T., 2007. Sedimentological signatures of the sub-Amery Ice Shelf circulation. *Antarctic Science* 19, 497-506.

Heroy, D., Sjunneskog, C., Anderson, J.B., 2008. Holocene climate change in the Bransfield Basin, Antarctic Peninsula: evidence from sediment and diatom analysis. *Antarctic Science* 20, 69–87, DOI: 10.1017/S0954102007000788.

Heroy, D.C., Anderson, J.B., 2005. Ice-sheet extent of the Antarctic Peninsula region during the Last Glacial Maximum (LGM) – Insights from glacial geomorphology. *Geological Society of America Bulletin* 117, 1497–1512.

Heroy, D.C., Anderson, J.B., 2007. Radiocarbon constraints on Antarctic Peninsula Ice Sheet retreat following the Last Glacial Maximum (LGM). *Quaternary Science Reviews* 26, 3286-3297.

Hillenbrand, C.-D., Baesler, A., Grobe, H. 2005. The sedimentary record of the last glaciation in the western Bellingshausen Sea (West Antarctica): Implications for the interpretation of diamictons in a polar-marine setting. *Marine Geology* 216, 191– 204, doi:10.1016/j.margeo.2005.01.007.

Hillenbrand, C.-D., Larter, R.D., Dowdeswell, J.A., Ehrmann W., Ó Cofaigh, C., Benetti, S., Graham, A.G.C., Grobe, H., 2010a. The sedimentary legacy of a palaeo-ice stream on the

shelf of the southern Bellingshausen Sea: Clues to West Antarctic glacial history during the Late Quaternary. *Quaternary Science Reviews* 29, 2741-2763.

Hillenbrand, C.-D., Smith, J.A., Kuhn, G., Esper, O., Gersonde, R., Larter, R.D., Maher, B., Moreton, S.G., Shimmield, T.M., Korte, M., 2010b. Age assignment of diatomaceous ooze deposited in the western Amundsen Sea Embayment after the Last Glacial Maximum. *Journal of Quaternary Science* 25, 280-295. <http://dx.doi.org/10.1002/jqs.1308>.

Hillenbrand, C.-D., Kuhn, G., Smith, J.A., Gohl, K., Graham, A.G.C., Larter, R.D., Klages, J.P., Downey, R., Moreton, S.G., Forwick, M., Vaughan, D.G., 2013. Grounding-line retreat of the West Antarctic Ice Sheet from inner Pine Island Bay. *Geology* 41, 35-38.

Jacobs, S.S., Hellmer, H.H., Jenkins, A., 1996. Antarctic ice sheet melting in the Southeast Pacific. *Geophysical Research Letters* 23, 957-960.

Jacobs, S.S., Jenkins, A., Giulivi, C.F., Dutrieux, P., 2011. Stronger ocean circulation and increased melting under Pine Island Glacier ice shelf. *Nature Geoscience* 4, 519-523.

Jakobsson, M., Anderson, J.B., Nitsche, F., Dowdeswell, J.A., Gyllencreutz, R., Kirchner, N., Mohammad, R., O'Regan, M., Alley, R.B., Anandakrishnan, S., Eriksson, B., Kirshner, A., Fernandez, R., Stollendorf, T., Minzoni, R., Majewski, W., 2011. Geological record of ice shelf break-up and grounding line retreat, Pine Island Bay, West Antarctica. *Geology* 39, 691-694.

Jakobsson, M., Anderson, J.B., Nitsche, F., Gyllencreutz, R., Kirshner, A., Kirchner, N., O'Regan, M., Mohammad, R., Eriksson, B., 2012. Ice sheet retreat dynamics inferred from glacial morphology of the central Pine Island Bay Trough, West Antarctica. *Quaternary Science Reviews* 38, 1-10.

Jakobsson, M., Nilsson, J., O'Regan, M., Backman, J., Löwemark, L., Dowdeswell, J.A., Mayer, L., Polyak, L., Colleoni, F., Anderson, L., Björk, G., Darby, D., Eriksson, B., Hanslik, D., Hell, B., Marcussen, C., Sellén, E., Wallin, Å., 2010. An Arctic Ocean ice shelf during MIS 6 constrained by new geophysical and geological data. *Quaternary Science Reviews* 13, 3505-3517. doi:10.1016/j.quascirev.2010.03.015

Jamieson, S.S.R., Vieli, A., Stokes, C.R., Ó Cofaigh, C., Livingstone, S.J., Hillenbrand, C.-D., in press. Understanding controls on rapid ice-stream retreat during the last deglaciation of Marguerite Bay, Antarctica, using a numerical model. *Journal of Geophysical Research, Earth Surface* 19, 247-263, doi:10.1002/2013JF002934.

Jenkins, A., Dutrieux, P., Jacobs, S.S., McPhail, S.D., Perrett, J.R., Webb, A.T., White, D., 2010. Observations beneath Pine Island Glacier in West Antarctica and implications for its retreat. *Nature Geoscience* 3, 468 – 472, doi:10.1038/ngeo890.

Johnson, J.S., Bentley, M.J., Smith, J.A., Finkel, R.C., Rood, D.H., Gohl, K., Balco, G., Larter, R.D., Schaefer, J.M. (2014). Rapid thinning of Pine Island Glacier in the early Holocene. *Science* 343, 999-1001.

Joughin, I., Smith, B.E., Holland, D.M., 2010. Sensitivity of 21st century sea level to ocean-induced thinning of Pine Island Glacier, Antarctica. *Geophysical Research Letters* 37, L20502, doi:10.1029/2010GL044819.

Joughin, I., Smith, B.E., Medley, B. 2014. Marine Ice Sheet Collapse Potentially under Way for the Thwaites Glacier Basin, West Antarctica. *Science* 344, 735-38.

Katz, R.F., Worster, G., 2010. Stability of ice-sheet grounding lines. *Proceedings of the Royal Society* 466, 1597–1620, doi:10.1098/rspa.2009.0434.

Kilfeather, A.A., Ó Cofaigh, C., Lloyd, J.M., Dowdeswell, J.D., Sheng, X., Moreton, S.G., 2011. Ice stream retreat and ice shelf history in Marguerite Trough, Antarctic Peninsula: sedimentological and foraminiferal signatures. *Geological Society of America Bulletin* 123, 997-1015.

King, M.A., Bingham, R.J., Moore, P., Whitehouse, P.L., Bentley, M.J., Milne, G.A., 2012. Lower satellite-gravimetry estimates of Antarctic sea-level contribution. *Nature* 491, 586-589.

Kirshner, A., Anderson, J.B., Jakobsson, M., O'Regan, M., Majewski, W., Nitsche, F., 2012. Post-LGM deglaciation in Pine Island Bay, West Antarctica. *Quaternary Science Reviews* 38, 11-26.

Klages, J.P. 2014. Late Quaternary West Antarctic Ice Sheet Dynamics: Remote sensing and substrate studies of palaeo-ice sheet bends on the Amundsen Sea shelf. PhD Thesis, University of Bremen, pp.188.

Klages, J.P., Kuhn, G., Hillenbrand, C.-D., Graham, A.G.C., Smith, J.A., Larter, R.D., Gohl, K., 2013. First geomorphological record and glacial history of an inter-ice stream ridge on the West Antarctic continental shelf. *Quaternary Science Reviews* 61, 47-61.

Larter, R.D., Gohl, K., Hillenbrand, C.-D., Kuhn, G., Deen, T.J., Dietrich, R., Eagles, G., Johnson, J.S., Livermore, R.A., Nitsche, F.O., Pudsey, C.J., Schenke, H.-W., Smith, J.A., Udintsev, G., Uenzelmann-Neben, G., 2007. West Antarctic Ice Sheet change since the last glacial period. *EOS* 88, 189-191.

Larter, R.D., Graham, A.G.C., Gohl, K., Kuhn, G., Hillenbrand, C.-D., Smith, J.A., Deen, T.J., Livermore, R.A., Schenke, H.-W., 2009. Subglacial bedforms reveal complex basal regime in a zone of paleo-ice stream convergence, Amundsen Sea Embayment, West Antarctica. *Geology* 37, 411–414.

Larter, R.D., Anderson, J.B., Graham, A.G.C., Gohl, K., Hillenbrand, C.D., Jakobsson, M., Johnson, J.S., Kuhn, G., Nitsche, F.O., Smith, J.A., Witus, A.E., Bentley, M.J., Dowdeswell, J.A., Ehrmann, W., Klages, J.P., Lindow, J., Ó Cofaigh, C., Spiegel, C., in press. Reconstruction of changes in the Amundsen Sea and Bellingshausen Sea sector of the West Antarctic Ice Sheet since the Last Glacial Maximum. *Quaternary Science Reviews* doi:10.1016/j.quascirev.2013.10.016.

LeMasurier, W.E. 2008. Neogene extension and basin deepening in the West Antarctic rift inferred from comparisons with the East African rift and other analogs. *Geology* 36, 247–250.

Licht, K.J., 2004. Antarctica's contribution to eustatic sea level during meltwater pulse-1A. *Sedimentary Geology* 165, 343–353.

Licht, K.J., Cunningham, W.L., Andrews, J.T., Domack, E.W., Jennings, A.E., 1998. Establishing chronologies from acid-insoluble organic <sup>14</sup>C dates on Antarctic (Ross Sea) and Arctic (North Atlantic) marine sediments. *Polar Research* 17, 203-216.

Licht, K.J., Dunbar, N.W., Andrews, J.T., Jennings, A.E., 1999. Distinguishing subglacial till and glacial marine diamictos in the western Ross Sea, Antarctica: implications for a Last Glacial Maximum grounding line. *Geological Society of America Bulletin* 111, 91-103.

Lowe, A.L., Anderson, J.B., 2002. Reconstruction of the West Antarctic ice sheet in Pine Island Bay during the Last Glacial maximum and its subsequent retreat history. *Quaternary Science Reviews* 21, 1879–1897.

McKay, R.M., Dunbar, G.B., Naish, T., Barrett, P.J., Carter, L., Harper, M., 2008. Retreat history of the Ross Ice Sheet (Shelf) since the Last Glacial Maximum from deep-basin sediment cores around Ross Island. *Palaeogeography, Palaeoclimatology, Palaeoecology* 260, 145-261.

Meyers, P. A., 1997. Organic geochemical proxies of paleoceanographic, paleolimnologic, and paleoclimatic processes. *Organic Geochemistry* 27, 213-250.

Nitsche, F.O., Jacobs, S.S., Larter, R.D., Gohl, K., 2007. Bathymetry of the Amundsen Sea Continental Shelf: Implications for Geology, Oceanography, and Glaciology. *Geochemistry, Geophysics, Geosystems* 8, Q10009, doi:10.1029/2007GC001694.

Nitsche, F.O., Gohl, K., Larter, R.D., Hillenbrand, C.-D., Kuhn, G., Smith, J.A., Jacobs, S., Anderson, J.B., Jakobsson, M., 2013. Paleo ice flow and subglacial meltwater dynamics in Pine Island Bay, West Antarctica. *Cryosphere* 7, 249-262 <http://dx.doi.org/10.5194/tc-7-249-2013>.

Ó Cofaigh, C., Dowdeswell, J.A., Allen, C.S., Hiemstra, J.F., Pudsey, C.J., Evans, J., Evans, D.J.A., 2005. Flow dynamics and till genesis associated with a marine-based Antarctic palaeo-ice stream. *Quaternary Science Reviews* 24, 709-740.

Park, J.W., Shepherd, A., Gourmelen, N., Kim, S.W., Vaughan, D.G., Wingham, D.J. 2013 Sustained retreat of the Pine Island Glacier. *Geophysical Research Letters* 40, 2137-2142. doi: 10.1002/grl.50379.

Payne, A. J., Vieli, A., Shepherd, A.P., Wingham, D.J., Rignot, E., 2004. Recent dramatic thinning of largest West Antarctic ice stream triggered by oceans. *Geophysical Research Letters* 31, L23401, doi:10.1029/2004GL021284.

Polyak, L., Jakobsson, M., 2011. Quaternary sedimentation in the Arctic Ocean: Recent advances and further challenges. *Oceanography* 24, 52–64, <http://dx.doi.org/10.5670/oceanog.2011.55>.

Post, A.L., Galton-Fenzi, B.K., Riddle, M.J., Herraiz-Borreguero, L., O'Brien, P.E., Hemer, M.A., McMinn, A., Rasch, D., Craven, M. 2014. Modern sedimentation, circulation and life beneath the Amery Ice Shelf, East Antarctica. *Continental Shelf Research* 74, 77–87.

Powell, R. D., 1994. Processes and facies of glacier grounding-line systems with inferences on lithofacies architecture and seismic stratigraphy. *Terra Antarctica* 1, 433-434.

Pritchard, H.D., Arthern, R.J., Vaughan, D.G., Edwards, L.A., 2009. Extensive dynamic thinning on the margins of the Greenland and Antarctic ice sheets. *Nature* 61, 971-975, doi:10.1038/nature08471.

Pritchard, H.D., Ligtenberg, S.R.M., Fricker, H.A., Vaughan, D.G., van den Broeke, M.R., Padman, L., 2012. Antarctic ice-sheet loss driven by basal melting of ice shelves. *Nature* 484, 502-505.

Pudsey, C. J., Evans, J. 2001. First survey of Antarctic sub-ice shelf sediments reveals mid-Holocene ice shelf retreat. *Geology* 29, 787-790.

Pudsey, C.J., Murray, J.W., Appleby, P., Evans, J., 2006. Ice shelf history from petrographic and foraminiferal evidence, Northeast Antarctic Peninsula. *Quaternary Science Reviews* 25, 2357-2379.

Rignot, E., 1998. Fast recession of a West Antarctic glacier. *Science* 281, 549– 551.

Rignot, E., Bamber, J.L., van den Broeke, M.R., Davis, C., Li, Y., van de Berg, W.J., van Meijgaard, E., 2008. Recent Antarctic ice mass loss from radar interferometry and regional climate modelling. *Nature Geoscience* 1, 106-110.

Schoof, C., 2007. Ice sheet grounding line dynamics: Steady states, stability and hysteresis. *Journal of Geophysical Research* 112, F03S28, doi:10.1029/2006JF000664.

Shepherd, A., Wingham, D., Rignot, E., 2004. Warm ocean is eroding West Antarctic Ice Sheet. *Geophysical Research Letters* 31, L23402.

Shepherd, A., Ivins, E.R., 45 others, 2012. A reconciled estimate of ice-sheet mass balance. *Science* 338, 1183-1189.

Smith, J.A., Hillenbrand, C.-D., Kuhn, G., Larter, R.D., Graham, A.G.C., Ehrmann, W., Moreton, S.G., Forwick, M., 2011. Deglacial history of the West Antarctic Ice Sheet in the western Amundsen Sea Embayment. *Quaternary Science Reviews* 30, 488-505.

Smith, J.A., Hillenbrand, C.-D., Larter, R.D., Graham, A.G.C., Kuhn, G., 2009. The sediment infill of subglacial meltwater channels on the West Antarctic continental shelf. *Quaternary Research* 71, 190-200.

Steig, E.J, Ding, Q., Battisti, D.S., Jenkins, A., 2012. Tropical forcing of Circumpolar Deep Water Inflow and outlet glacier thinning in the Amundsen Sea Embayment, West Antarctica. *Annals of Glaciology* 53 (60), 19-28.

Stuiver, M., Reimer, P.J., Reimer, R.W., 2005. CALIB 5.0 (<http://calib.qub.ac.uk/calib/manual/>).

Tinto, K.J., Bell, R.E., 2011. Progressive unpinning of Thwaites glacier from newly identified offshore ridge: constraints from aerogravity. *Geophysical Research Letters* 38, L20503. <http://dx.doi.org/10.1029/2011GL049026>.

Thoma, M., Jenkins, A., Holland, D., Jacobs, S.S., 2008. Modelling Circumpolar Deep Water intrusions on the Amundsen Sea continental shelf, Antarctica. *Geophysical Research Letters* 35, L18602, doi:10.1029/2008GL034939.

Walker, D. P., Brandon, M.A., Jenkins, A., Allen, J.T., Dowdeswell, J.A., Evans, J., 2007. Oceanic heat transport onto the Amundsen Sea shelf through a submarine glacial trough. *Geophysical Research Letters* 34, L02602, doi:10.1029/2006GL028154.

Winberry, J.P., Anandakrishnan, S., 2004. Crustal structure of the West Antarctic rift system and Marie Byrd Land hotspot. *Geology* 32, 977–980.

## Figures and Tables

Figures 1. Map of the Amundsen Sea Embayment (ASE) showing locations of sediment cores and surface sediment samples (black circles) and regional bathymetry (Nitsche *et al.*, 2007). Sediment cores were recovered along transects in the Pine Island-Thwaites (PIT) trough, Pine Island-Thwaites east (PITE) and west troughs (PITW) and Cosgrove and Abbot Troughs (black arrows). The locations of additional cores referred to in the text are also show. Blue circle=Kirshner *et al.* (2012); Lowe and Anderson, (2002); green circles= Klages *et al.* (2013); red circles=Hillenbrand *et al.* (2013). Black arrows indicate flow directions of palaeo-ice streams. Geomorphological evidence in the form of contiguous grounding zone wedges in the Abbot (GZWa and GZWb; Klages, 2014) and PITPIS/PITE troughs (GZW1-5; Graham *et al.*, 2010) suggest that the ice margin stepped back uniformly. Cores either side of the trough axis (A-A' profile) were projected onto the centre line (grey dashed lines) to calculate distance from the grounding line (from 2000). (B) Inset shows location of Amundsen Sea (WAIS=West Antarctic Ice Sheet).

Figure 2. Representative core logs and core data from the eastern ASE, showing simplified lithology, shear strength (green line, closed black circles), water content (blue line, open triangles), magnetic susceptibility (measured with the MSCL; red line), contents of mud (0-63  $\mu\text{m}$ ; white fill), sand (63  $\mu\text{m}$ -2 mm; grey fill) and gravel (>2 mm; black fill), organic carbon ( $C_{\text{org}}$ ) (blue line, open triangles), C/N (black line, closed circles), clay mineral data (smectite/chlorite ratio) and  $\text{CaCO}_3$  data (orange line, open squares). Uncorrected (black circles) and calibrated (red circles)  $^{14}\text{C}$  ages are also shown (with the deglacial ages highlighted in orange) together with a facies log (right numbered panel). Crossed circles represent foraminiferal  $^{14}\text{C}$  ages.

Figure 3. Map of uncorrected surface  $^{14}\text{C}$  ages (AIO: black font; foraminifera: red font) from the eastern Amundsen Sea shelf. Note that younger  $^{14}\text{C}$  ages are concentrated along the eastern coastline, and specifically along the Cosgrove-Abbot trough (grey lines). In contrast, surface ages along the main Pine Island-Thwaites (PIT) trough are typically much older (see text for discussion). PITE, PITW =Pine Island Thwaites east and west troughs respectively.

Figure 4. Uncorrected surface  $^{14}\text{C}$  ages of AIO samples versus kaolinite (a) and  $\delta^{13}\text{C}$  (b).

Figure 5. (a) Calibrated  $^{14}\text{C}$  deglacial ages versus distance from modern grounding line (GL) and (b) with obvious outliers removed. Unless shown, size of marker encompasses  $1\sigma$  error.

Distance was calculated along a centre line shown in Figure 1. Cores to the east and west of this are projected to the centre line to calculate distance from GL.

Figure 6. Compilation of deglacial dates from the eastern ASE (this study – black filled squares) and western ASE (grey open circles) together with dates from Kirshner *et al.* (2012) (blue filled circles), Lowe and Anderson (2002) (open blue circles), Klages *et al.* (2013) (green filled circles) and Hillenbrand *et al.* (2013) (red filled triangles). Error bars incorporate  $1\sigma$  (calibration) error, and the range of dated samples. If no error bar is shown, the size of the marker represents the total error. Calibrated ages are plotted against distances from the modern grounding line (GL), which have been normalised using the distance between the GL and the shelf edge.

Figure 7. (a) Calculated retreat rates for two 'retreat trajectories (A & B)' for the eastern Amundsen Sea, incorporating deglacial data from this study (black squares), Kirshner *et al.* (2012) (blue filled circles) and Hillenbrand *et al.* (2013) (red filled triangles). (b) Shows calculated retreat rates and along trough profile (A-A' in Figure 1) together with the positions (projected onto the trough profile) of relevant cores and grounding zone wedges (GZW) 1-5 (Graham *et al.*, 2009). The trough profile was extracted from a combined multibeam (50 m) and regional (3 km) bathymetric grid (Nitsche *et al.*, 2007).

Table 1: Site information on sediment cores from the eastern ASE. VC = vibro-core; BC=box core; GBC = giant boxcore; GC = gravity core.

Table 2: Uncorrected, corrected and calibrated AMS  $^{14}\text{C}$  dates from the eastern ASE together with locations, sample depth and dated material (AIO = acid insoluble organic matter, pF = planktonic foraminifera, bF= benthic foraminifera, C=corals, Bz= bryozoans). A marine reservoir effect (= MRE) correction of  $1300 \pm 70$  years (Berkman and Forman, 1996) is used. AIO down-core ages were corrected by subtracting the uncorrected seafloor surface AIO age from a box core recovered at the same or a nearby site, or by subtracting the uncorrected AIO core-top age from the same core (termed the local contamination offset (LCO)). We show the entire  $1\sigma$  range for each calibrated age (Min, Max), but quote the mean age throughout the text. Dates assumed to mark the minimum ages of GL retreat from the core sites are shown in bold. AMS  $^{14}\text{C}$  dating was carried out at the NERC Radiocarbon Laboratory (Environment) in East Kilbride (UK), and BETA Analytic Inc., Miami, Florida, U.S.A. (with prefix SUERC and BETA).

\*Denotes calibration using Fairbanks calibration curve

(<http://radiocarbon.ldeo.columbia.edu/research/radcarbcal.htm>) for samples older than 25,000  $^{14}\text{C}$  yr BP (Fairbanks *et al.*, 2005).

\*\*Published in Hillenbrand *et al.* (2013).

Table 3: Calibrated deglacial ages for the Amundsen Sea Embayment providing an upper and lower estimate for the minimum age of GL retreat. Dates from Hillenbrand *et al.* (2013) and Kirshner *et al.* (2012) were recalibrated using an MRE correction of  $1300 \pm 70$  years. Also listed are the deglacial ages (1-9) for the western ASE (see Table 3 in Smith *et al.* 2011 for details).

ACCEPTED MANUSCRIPT

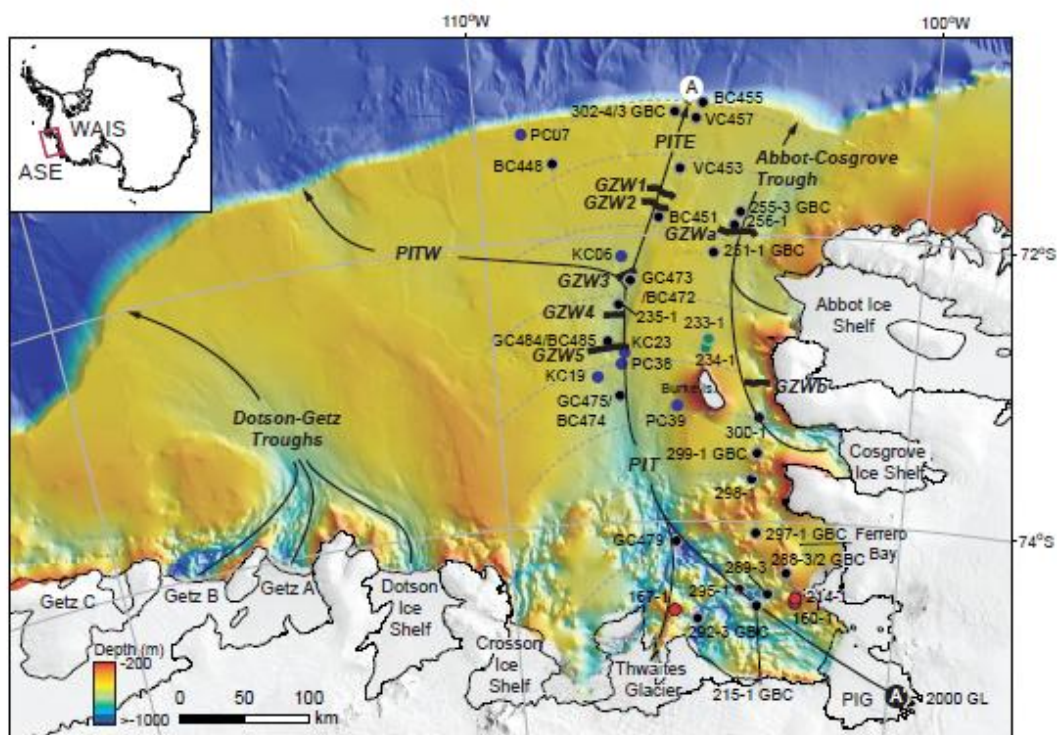


Figure 1

ACC

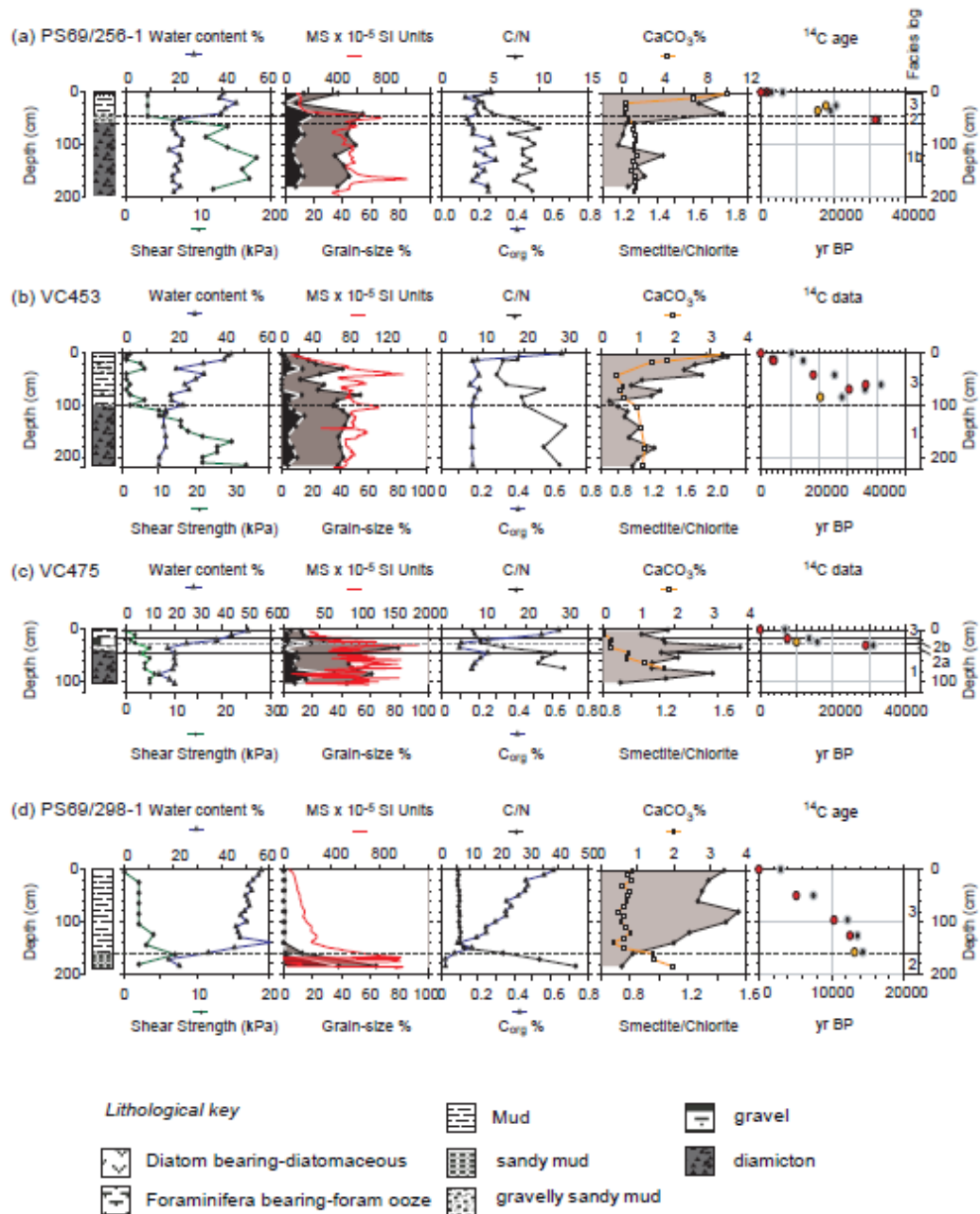


Figure 2

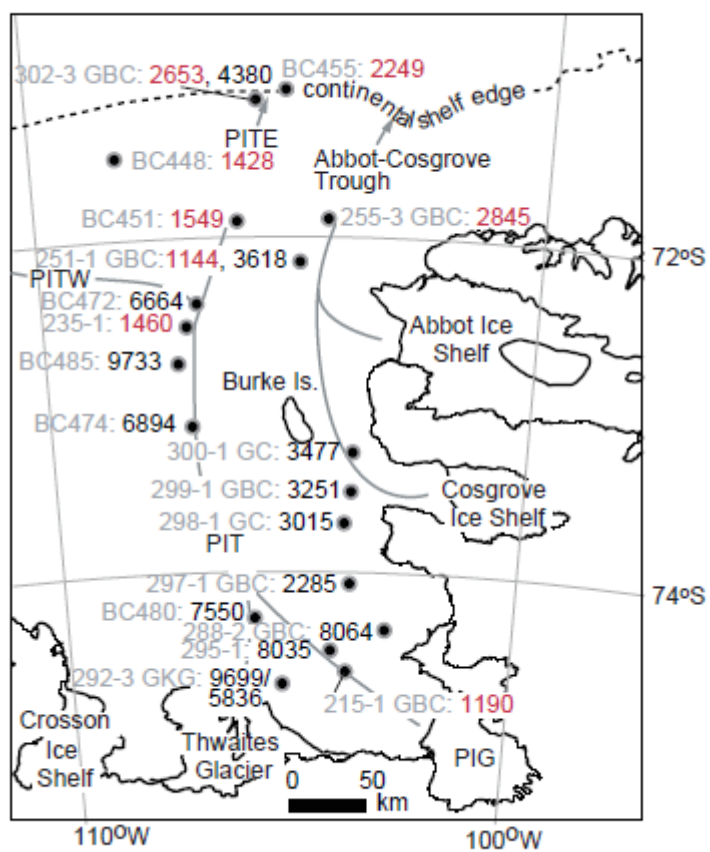


Figure 3

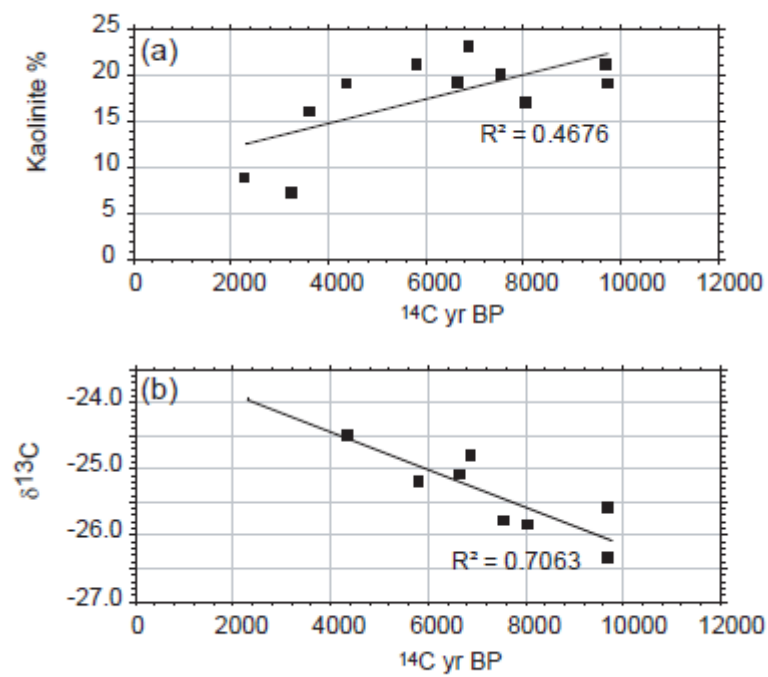


Figure 4

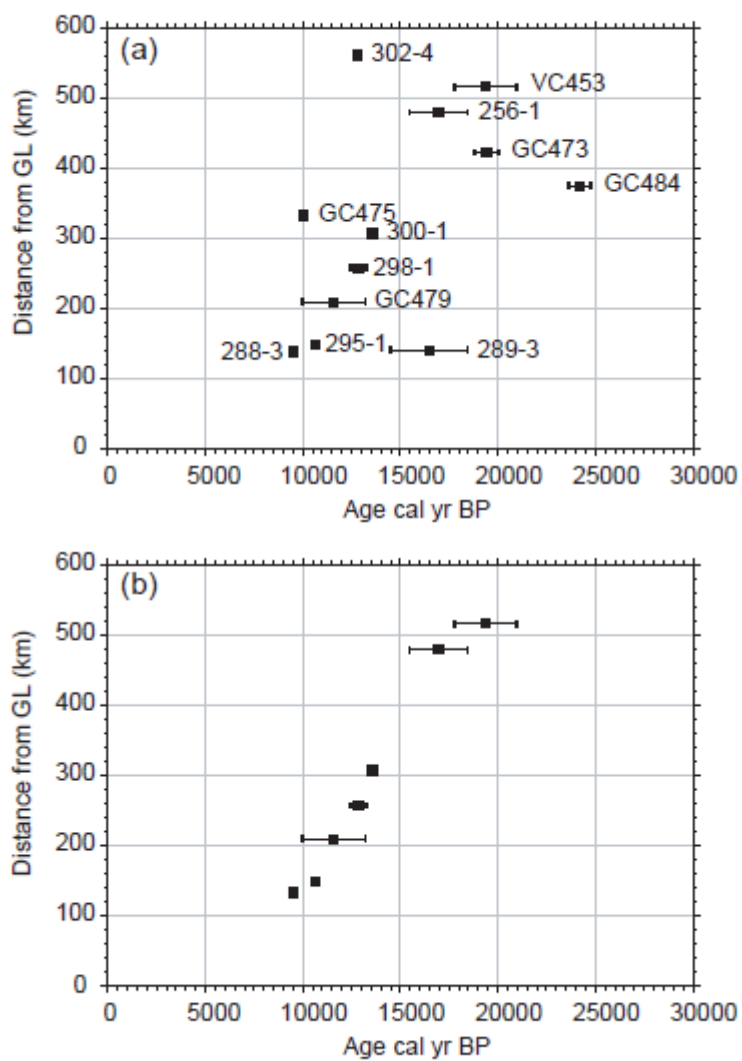


Figure 5

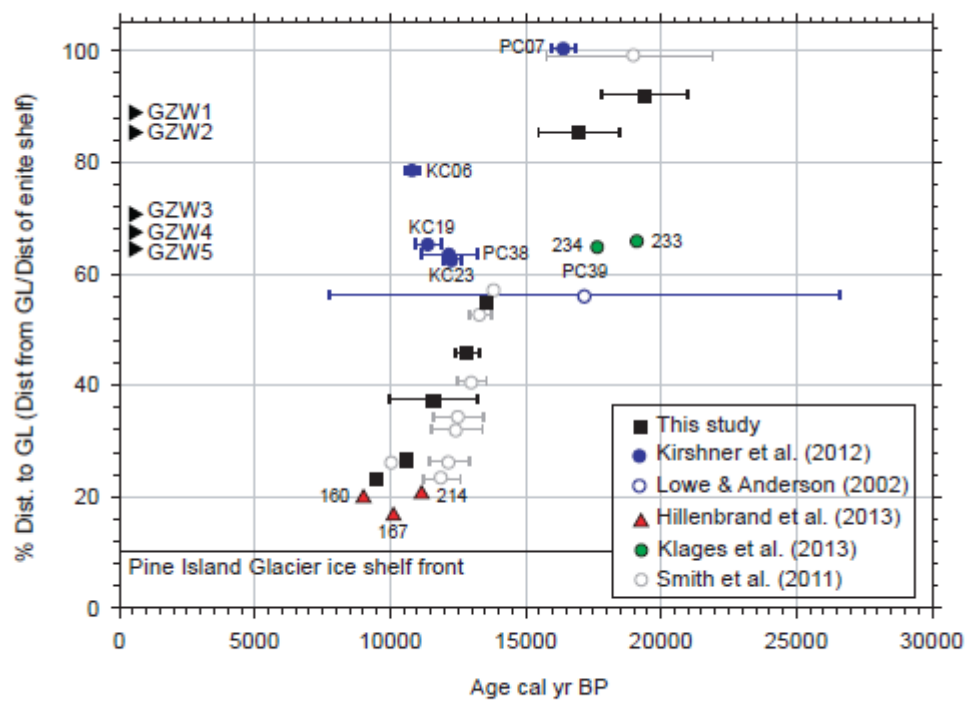


Figure 6

ACCEPTED

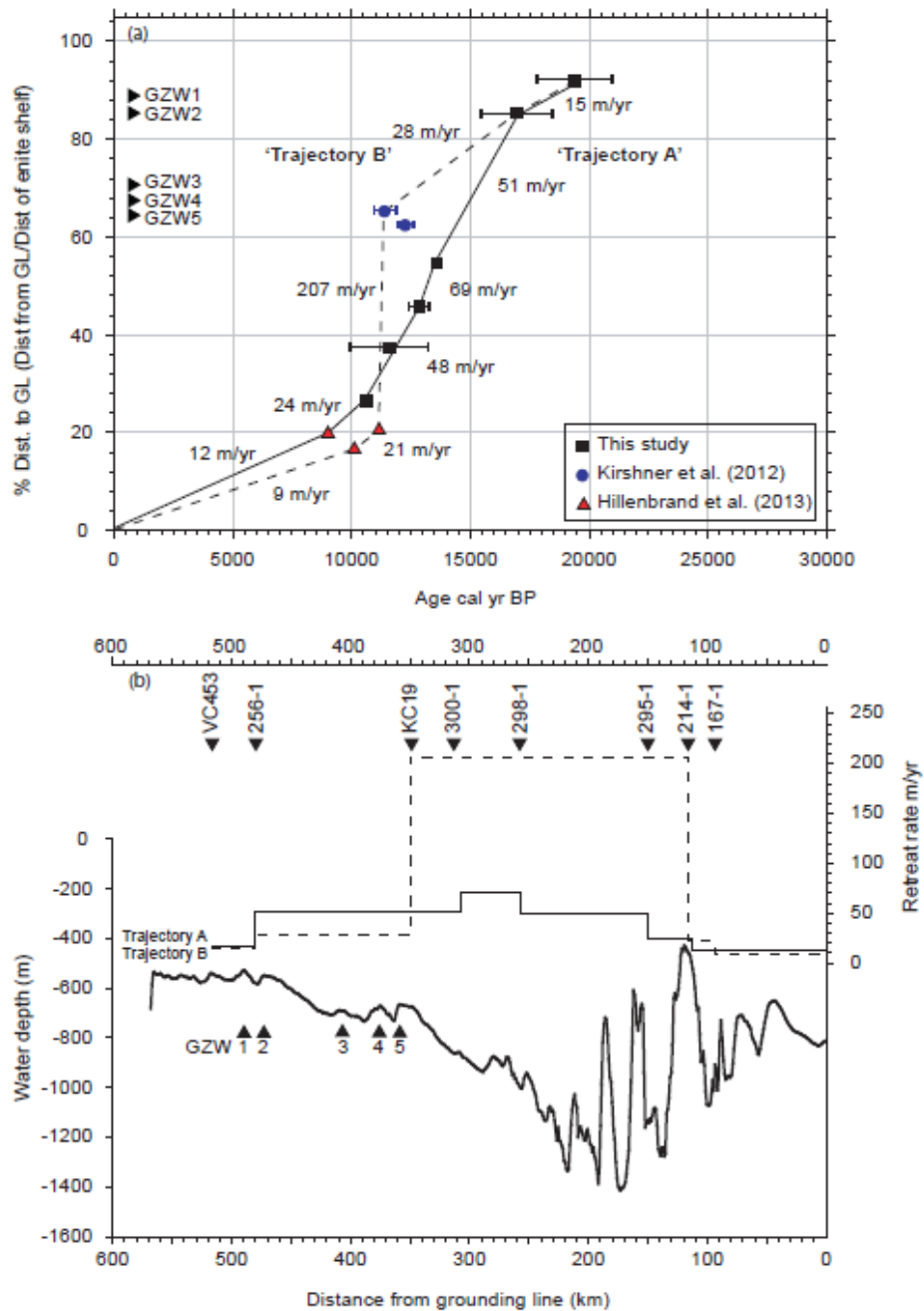


Figure 7

Table 1

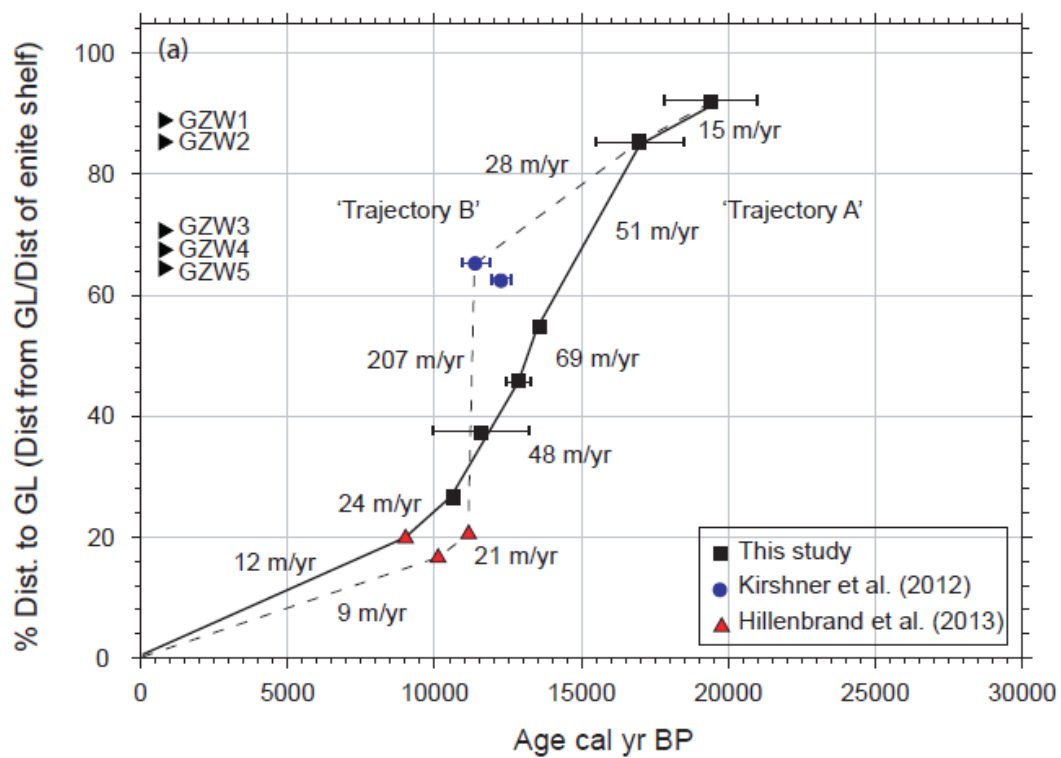
Core	Expedition [year]	Water Depth (m)	Latitude deg.S	Longitude deg. W	Core Recovery (m)
BC448	JR141 [2006]	488	-71.46828	-108.35893	0.12
BC451	JR141 [2006]	568	-71.86563	-106.04084	0.24
BC455	JR141 [2006]	807	-71.06779	-105.07978	0.16
VC453	JR141 [2006]	587	-71.52646	-105.55266	2.17
VC457	JR141 [2006]	538	-71.17562	-105.19194	1.32
BC472	JR179 [2008]	702	-72.30270	-106.71920	0.3
GC473	JR179 [2008]	702	-72.30280	-106.71920	2.09
BC474	JR179 [2008]	760	-73.10730	-107.04820	0.2
GC475	JR179 [2008]	760	-73.10730	-107.04820	1.05
BC480	JR179 [2008]	1452	-74.13780	-105.74000	0.23
GC479	JR179 [2008]	1453	-74.13780	-105.74000	1.325
BC485	JR179 [2008]	692	-72.72530	-107.29400	0.31
GC484	JR179 [2008]	692	-72.72530	-107.29400	2.04
PS75/215-1 GBC	ANT-XXVI/3 [2010]	556	-74.59170	-104.04200	0.62
PS75/235-1 GBC	ANT-XXVI/3 [2010]	752	-72.66580	-107.16550	0.4
PS69/251-1 GBC	ANT-XXIII/4 [2006]	573	-72.11420	-104.80520	0.38
PS69/255-3 GBC	ANT-XXIII/4 [2006]	654	-71.79720	-104.36120	0.33
PS69/256-1 GC	ANT-XXIII/4 [2006]	668	-71.92250	-104.33780	1.96
PS69/288-2 GBC	ANT-XXIII/4 [2006]	773	-74.41520	-102.99200	0.44
PS69/288-3 GC	ANT-XXIII/4 [2006]	772	-74.41570	-102.99130	9.12
PS69/289-3 GC	ANT-XXIII/4 [2006]	943	-74.50700	-103.35920	6.11
PS69/292-3 GBC	ANT-XXIII/4 [2006]	1406	-74.68250	-105.19330	0.36
PS69/295-1 GC	ANT-XXIII/4 [2006]	1151	-74.47880	-104.10150	4.86
PS69/297-1 GBC	ANT-XXIII/4 [2006]	481	-74.07980	-103.66770	0.36
PS69/298-1 GC	ANT-XXIII/4 [2006]	922	-73.70220	-103.83250	1.9
PS69/299-1 GBC	ANT-XXIII/4 [2006]	718	-73.44370	-103.64820	0.39
PS69/300-1 GC	ANT-XXIII/4 [2006]	766	-73.27050	-103.67930	1.41
PS69/302-3 GBC	ANT-XXIII/4 [2006]	565	-71.13020	-105.65070	0.27
PS69/302-4 GC	ANT-XXIII/4 [2006]	564	-71.13000	-105.64980	1.56

Table 2

Core	Publication Code	Depth (cmbsf)	Material Dated	<sup>14</sup> C Age (yr BP)	±1σ	δ <sup>13</sup> C	C/N	Kaol.	LCO	MRE	Cal. yr BP			±1σ
											Min.	Max.	Mean	
BC448**	SUERC-18332	0.5	pF	1428	37	0.20	-	21.0	-	1300	1	258	130	107
BC451**	SUERC-18938	0.5	pF	1549	35	0.70	-	16.0	-	1300	147	421	284	106
BC455	SUERC-18941	0.5	pF	2249	37	1.00	-	16.0	-	1300	768	999	884	107
VC453	SUERC-27747	0.5	AIO	10667	45	-25.6	14.2	14.2	10667	-	-	-	N/A	N/A
VC453	SUERC-18945	13	pF	4799	38	0.80	18.2	18.2	-	1300	3715	4015	3865	107
VC453	SUERC-27747	14.5	AIO	14648	45	-25.6	18.2	18.2	10667	1300	4414	4520	4467	110
VC453	BETA-295157	42	AIO	25490	130	-24.1	22.1	22.1	10667	1300	17810	18481	18146	164
VC453	SUERC-27749	60.5	AIO	41543	1695	-24.9	24.5	24.5	10667	1300	-	-	36260*	1698
VC453	BETA-295158	69.5	AIO	36040	300	-24.7	21.3	21.3	10667	1300	-	-	30523*	316
VC453	SUERC-27750	84.5	AIO	28091	315	-25.0	23.9	23.9	10667	1300	20208	20972	<b>20590</b>	330
VC457	SUERC-18946	4	pF	2348	37	0.90	-	-	-	1300	896	1128	1012	107
BC472Y	SUERC-27751	0.5	AIO	6664	38	-25.1	19.2	19.2	6664	-	-	-	N/A	N/A
GC473	BETA-295159	16	AIO	14040	60	-23.7	20.7	20.7	6664	1300	8067	8315	8191	117
GC473	SUERC-27754	18.5	AIO	22384	156	-	27.3	27.3	6664	1300	18822	19066	<b>18944</b>	185
GC473	BETA-295160	25	AIO	23420	110	-23.7	24.0	24.0	6664	1300	19632	20058	<b>19845</b>	149
GC473	SUERC-27755	59.5	AIO	41657	1721	-25.1	24.9	24.9	6664	1300	-	-	40285	1724
BC474X	SUERC-27410	0.5	AIO	6894	38	-24.8	19.8	23.0	6894	-	-	-	N/A	N/A
GC475	SUERC-27756	17.5	AIO	13579	57	-24.5	22.7	22.7	6894	1300	7505	7606	7556	115
GC475	BETA-295161	24	AIO	15820	60	-23.4	26.0	26.0	6894	1300	9929	10186	<b>10058</b>	117
GC475	SUERC-27757	30.5	AIO	31294	476	-	26.0	26.0	6894	1300	-	-	29223*	486
BC480X	SUERC-27413	0.5	AIO	7550	38	-25.8	-	20.0	7550	-	-	-	N/A	N/A
GC479	SUERC-27411	60.5	AIO	11162	47	-23.3	-	-	7550	1300	3860	3979	3920	110
GC479	SUERC-27412	117.5	AIO	18776	99	-24.6	-	-	7550	1300	13038	13226	<b>13132</b>	141
GC479	BETA-295162	120	AIO	16580	70	-24.1	-	-	7550	1300	9960	10258	<b>10109</b>	122
BC485Y	SUERC-26022	0.5	AIO	9733	43	-26.4	-	19.0	9733	-	-	-	N/A	N/A
GC484	BETA-295163	19	AIO	12700	50	-23.8	19.5	19.5	9733	1300	3067	3241	3154	112
GC484	BETA-295164	23.5	AIO	13510	60	-23.8	21.2	21.2	9733	1300	4006	4243	4125	117
GC484	SUERC-26023	32.5	AIO	29917	397	-24.7	26.9	26.9	9733	1300	23625	24763	24194	409
GC484	SUERC-26024	57.5	AIO	40644	1514	-25.0	35.6	35.6	9733	1300	-	-	36297*	1517
PS75/215-1 GBC**	Beta-315966	0.5	Bz	1190	30	-	-	-	-	1300	-	-	N/A	N/A
PS75/235-1 GC**	Beta-284613	0.5	C	1460	40	-	-	-	-	1300	1	287	145	100
PS69/251-1 GBC**	SUERC-18942	0.5	pF	1144	37	0.90	-	16.0	-	1300	-	-	N/A	N/A
PS69/251-1 GBC	SUERC-11790	0.5	AIO	3618	35	-	-	16.0	3618	1300	-	-	N/A	N/A
PS69/255-3 GBC**	SUERC-18943	0.5	pF	2845	37	0.90	-	14.0	-	1300	1369	1615	1492	107
PS69/256-1 GC	SUERC-21909	0.5	AIO	6018	39	-25.5	25.4	13.7	6018	-	-	-	N/A	N/A
PS69/256-1 GC	SUERC-21910	26.5	AIO	20758	131	-25.5	25.0	13.4	6018	1300	17547	18426	<b>17987</b>	165
PS69/256-1 GC	BETA-295167	36	AIO	19280	120	-24.6	6.1	13.5	6018	1300	15475	15948	<b>15712</b>	156
PS69/256-1 GC	SUERC-21911	53.5	AIO	32392	544	-24.5	17.7	15.3	6018	1300	-	-	31623	553
PS69/288-3 GC	BETA-338486	318	pF, bF	8740	50	-	-	-	-	1300	8177	8402	8290	112
PS69/288-3 GC	BETA-337427	338	pF, bF	8640	40	-1.3	-	-	-	1300	8101	8330	8216	108
PS69/288-3 GC	BETA-331574	398	pF, bF	8720	40	-1.3	-	-	-	1300	8171	8383	8277	108
PS69/288-3 GC	BETA-337428	458	pF, bF	9020	40	-1.6	-	-	-	1300	8447	8749	<b>8598</b>	108
PS69/288-2 GBC	SUERC-27414	0.5	AIO	8064	41	-25.8	-	17.0	8064	-	-	-	N/A	N/A
PS69/289-3 GC	BETA-295168	255	AIO	22870	100	-23.9	11.1	19.7	8064	1300	17767	18460	18114	141
PS69/289-3 GC	SUERC-27415	330.5	AIO	20668	124	-24.8	8.5	18.9	8064	1300	14496	15067	14782	159
PS69/289-3 GC	SUERC-28182	400.5	AIO	29661	384	-24.6	9.4	19.7	8064	1300	-	-	25942*	397
PS69/289-3 GC	SUERC-27416	567.5	AIO	29012	354	-24.6	9.3	19.6	8064	1300	24651	25609	25130	368
PS69/292-3 GBC_1	SUERC-12115	0.5	AIO	9699	41	-25.6	-	21.0	5836	1300	4236	4406	4321	108
PS69/292-3 GBC_2	SUERC-28183	0.5	AIO	5836	36	-25.2	-	21.0	5836	1300	-	-	-	106
PS69/295-1 GC	SUERC-26019	0.5	AIO	8035	38	-25.3	6.0	17.0	8035	-	-	-	N/A	N/A
PS69/295-1 GC	BETA-295169	101	AIO	14050	60	-24.1	6.7	16.1	8035	1300	6787	6939	6863	117
PS69/295-1 GC	BETA-295170	119	AIO	17430	70	-23.7	8.5	17.4	8035	1300	10520	10710	<b>10615</b>	122
PS69/295-1 GC	SUERC-26020	126	AIO	22279	152	-24.3	8.3	17.4	8035	1300	16736	17359	17048	182
PS69/295-1 GC	SUERC-26021	253	AIO	29288	366	-24.2	12.5	32.6	8035	1300	-	-	25473	379
PS69/297-1 GBC	SUERC-11796	0.5	AIO	2285	35	-27.4	-	9.0	2285	-	-	-	N/A	N/A
PS69/298-1 GC	SUERC-28186	0.5	AIO	3015	36	-25.9	6.0	9.7	3015	-	-	-	N/A	N/A
PS69/298-1 GC	SUERC-27759	50.5	AIO	7548	39	-26.5	6.1	10.1	3015	1300	5065	5307	5186	107
PS69/298-1 GC	SUERC-27760	97.5	AIO	12267	50	-25.5	5.5	8.2	3015	1300	10299	10510	10405	112
PS69/298-1 GC	SUERC-27761	127.5	AIO	13623	56	-25.3	5.4	8.1	3015	1300	12419	12782	<b>12601</b>	115
PS69/298-1 GC	SUERC-27764	159	AIO	14367	62	-	11.7	8.3	3015	1300	13172	13281	<b>13227</b>	118
PS69/299-1 GBC	SUERC-11797	0.5	AIO	3251	35	-	-	7.0	3251	-	-	-	N/A	106
PS69/300-1 GC	SUERC-27765	0.5	AIO	3477	37	-25.9	5.7	6.9	3477	-	-	-	N/A	N/A
PS69/300-1 GC	SUERC-28187	28.5	AIO	9212	40	-25.6	5.4	7.1	3477	1300	6474	6625	6550	108
PS69/300-1 GC	SUERC-28188	58.5	AIO	15205	68	-25.3	6.1	6.8	3477	1300	13480	13670	<b>13575</b>	121
PS69/300-1 GC	SUERC-27766	78.5	AIO	22244	154	-	12.4	9.9	3477	1300	22189	22451	22320	184
PS69/302-3 GBC	SUERC-26717	0.5	pF	2653	37	0.3	-	19.0	-	1300	1184	1407	1296	107
PS69/302-3 GBC	BETA-295171	1.5	AIO	4380	40	-24.5	-	19.0	4380	-	-	-	N/A	N/A
PS69/302-4 GC	SUERC-26718	15	pF	9850	37	0.3	3.9	17.6	-	1300	9493	9770	9632	107
PS69/302-4 GC	BETA-295172	21	AIO	15180	60	24.6	3.6	16.6	4380	1300	12801	12859	<b>12830</b>	117

Table 3

Core/Map ID	Lat.	Long.	Distance GL (km)	Dist% (Fig. 6)	Deglacial age cal. yr BP			Source
					Mid	min	max	
VC453	-71.5265	-105.5527	516	92	19391	17810	20972	This study
PS69/256-1 GC	-71.9225	-104.3378	479	85	16969	15475	18462	
PS69/300-1 GC	-73.2705	-103.6793	307	55	13575	13480	13670	
PS69/298-1 GC	-73.7022	-103.8325	257	46	12850	12419	13281	
VC479	-74.1378	-105.7400	209	37	11593	9960	13226	
PS69/295-1 GC	-74.4788	-104.1015	149	27	10615	10520	10710	
PS75/160-1 GC	-74.5638	-102.6240	111	20	9015	8764	9266	Hillenbrand et al. (2013)
PS75/167-1 GC	-74.6228	-105.8018	93	17	10124	9855	10393	
PS75/214-1 GC	-74.5327	-102.6213	115	21	11157	10909	11405	
PC38	-72.9730	-107.5680	355	63	12193	11148	13238	Kirshner et al. (2012)
KC19	-73.1285	-106.9688	349	62	12289	11958	12619	
1	-71.8136	-117.4335	340	99	19247	16036	22457	Smith et al. (2011)
2	-73.1425	-115.7044	196	57	13850	13579	13915	
3	-73.2371	-114.3391	181	53	13325	12900	13750	
4	-73.4469	-115.1981	139	40	13025	12500	13550	
5	-73.6689	-114.9780	118	34	12525	11600	13450	
6	-73.7029	-115.4860	110	33	12450	11500	13400	
7	-73.856	-117.776	90	32	12175	11450	12900	
8	-73.962	-117.843	80	23	11900	11200	12600	
9	-73.8958	-115.9311	89	26	9936	10207	10072	



Graphical abstract

ACCEPTED

## Highlights

- We provide a comprehensive deglacial chronology for the eastern Amundsen Sea
- Data will help constraints ice sheet models
- Shows consistent pattern of deglaciation across the Amundsen Sea Embayment
- Pattern of retreat highlights the importance of reverse bedslopes

ACCEPTED MANUSCRIPT